March 2020
Cowlitz Restoration and Recovery Habitat Assessment

# Hydrodynamic Modeling and Habitat Suitability Assessment – Final Report

Prepared for Tacoma Power

March 2020
Cowlitz Restoration and Recovery Habitat Assessment

# Hydrodynamic Modeling and Habitat Suitability Assessment – Final Report

**Prepared for**
Tacoma Power
3628 South 35th Street
Tacoma, Washington 98409

**Prepared by**
Anchor QEA, LLC
1605 Cornwall Avenue
Bellingham, Washington 98255

Project Number: 180479-06.01
B:\Projects\Tacoma Power\Cowlitz_Restoration_and_Recovery\Deliverables\Report\FINAL Modeling and Habitat Assessment Report\CRR Habitat Assessment - Final Modeling Report - 2020-03-31.docx

# TABLE OF CONTENTS

## TABLES



## FIGURES

## APPENDIX

# ABBREVIATIONS

| | |
|---|---|
| cfs | cubic feet per second |
| CRR | Cowlitz Restoration and Recovery |
| FEMA | Federal Emergency Management Agency |
| FIS | Flood Insurance Study |
| fps | feet per second |
| HSI | Habitat Suitability Index |
| LCPUD | Lewis County Public Utility District |
| LiDAR | Light Detection and Ranging |
| NAVD88 | North American Vertical Datum of 1988 |
| NGVD29 | National Geodetic Vertical Datum of 1929 |
| NLCD | National Land Cover Database |
| psf | pounds per square foot |
| QSI | Quantum Spatial, Inc. |
| RCI | River Complexity Index |
| SCE | Standardized Complexity Evaluation |
| SR-12 | State Route 12 |
| USACE | U.S. Army Corps of Engineers |
| USGS | U.S. Geological Survey |
| WDFW | Washington Department of Fish and Wildlife |

# 1 Introduction and Purpose

Anchor QEA, LLC, was selected by Tacoma Power to develop a baseline hydrodynamic model of the upper Cowlitz River and floodplain to support the Cowlitz Restoration and Recovery (CRR) Habitat Assessment.

The following list outlines Anchor QEA's scope of services for this project:

**Anchor QEA Scope of Services:**

Task 1: Development of a Coarse-Level Hydraulic Model

- 1D HEC-RAS hydraulic model, developed based on the extents of the topo-bathymetric Light Detection and Ranging (LiDAR) data provided by Tacoma Power
- Evaluation of basic system hydraulics

Task 2: Development of a Fine-Scale Hydraulic Model

- 2D HEC-RAS model, developed for Randle to Packwood and appended to the 1D model section (Lake Scanewa to Randle).
- Simulation of average summer flow, average winter flow, annual flood event, 2-year flood event, and 10-year flood event flows
- Evaluation of channel complexity
- Evaluation of preliminary habitat restoration alternative (to be completed)

Task 3: Habitat Suitability Evaluation

- Habitat Suitability Index (HSI), computed based on predicted water depth and depth-averaged velocity

Task 4: Mapping and Reporting

- Web maps of predicted hydraulics (depth and depth-averaged velocity) and HSI results
- Summary Report
- 1D- and 2D-model files and results files

# 2 Site Location and History

The extents of this investigation were the upper Cowlitz River basin, located in eastern Lewis County, Washington. The upper Cowlitz River flows into Lake Scanewa, at the western extents of the study area, which is an artificial lake with water levels controlled by the Cowlitz Falls Hydroelectric Dam. The dam is operated by Lewis County Public Utility District (LCPUD). The upstream extents of the study are approximately 2 miles downstream of Packwood, Washington, which is the upstream-most extents of the 2018 aerial topo-bathymetric LiDAR survey provided by Tacoma Power for this work.

Hydraulically, the backwater influence from Lake Scanewa extends approximately 6 miles upstream of the Cowlitz Falls Dam, and flows are generally confined within the channel banks, even during flood events. Therefore, the predicted hydraulics and HSI were not further evaluated as part of this study in the 1D reach of the model downstream of Randle. This section of the model remained in the model to serve as the downstream boundary conditions for the three areas of interest.

The focus areas of this modeling effort were divided into three general areas of focus: lower river valley areas near Randle, the middle river valley areas upstream of Randle, and the areas near Packwood upstream of the State Route 12 (SR-12) bridge (Figure 4-1). The Randle hydraulic area extends from approximately 3 miles downstream of Randle to approximately 1 mile upstream of Randle. This section of the river is characterized by a very wide floodplain (1 to 3 miles) and a highly meandering and mostly single-threaded channel. The middle river valley area is characterized by a wide floodplain (up to 1 mile) and a highly meandering channel with areas of rapid channel migration and erosion. There are numerous former avulsion channels that backwater during high flows. Silver Creek, which is the largest tributary within the model domain, occurs in this stretch of the model. The upstream area of the model is the area of the model upstream of SR-12. This reach is characterized by sections of confined channel and many unconfined areas where the channel has previously avulsed. This reach shows rapid erosion of existing channel banks and rapid avulsion of the main flow channel based on a comparison of aerial photography to the location of the channel based on LiDAR.

Near Randle, Washington, and extending upstream to the SR-12 crossing near Cora, Washington, the main channel is highly meandering, and the basin floodplain is very wide (1 to 3 miles wide). Significant flooding has been a recurring problem in the reaches between Randle and SR-12. The river basin above Randle has numerous depressions in the floodplain from former avulsion channels, and channel migration can occur rapidly in areas, with erosional hotspots on riverbends. Significant bank erosion near SR-12 has required extensive armoring to avoid loss of the road. Upstream of SR-12, the river grade steepens, and the flows seem to alternate between areas of wide and narrow channels, along with areas of multiple former avulsion channels. Channel migration occurs rapidly in this area, as seen in historical imagery. Channels in flow paths in this area were noted in the 2018 LiDAR data when compared to the latest Google Earth Imagery from 2015.

# 3 Goals and Objectives

The goal of this study was to develop a modeling framework that could be used to support the CRR Program, including planning habitat protection and restoration in the upper Cowlitz River basin. Initially, a coarse-scale model was developed to better inform the targeted reaches for development of a refined 2D model. The refined model was developed for 24 miles of the river and floodplain basin, from 3 miles downstream of Randle upstream to approximately 2 miles south of Packwood, Washington. The hydraulic predictions from the fine-scale 2D model were then used for the following applications:

- Predictions of channel hydraulics during typical average summer and winter flows when flows are generally confined within the river banks
- Predictions of flooding extents, with depths and velocities, during the 1-, 2-, and 10-year return interval flood event, and to gain a better understanding of how the range of flows in the system affect floodplain connectivity
- Identification (Calculation?) of HSI for juvenile steelhead (*Oncorhynchus mykiss*) and juvenile Chinook salmon (*O. tshawytscha*) species
- Channel complexity evaluation for the extents of the fine-scale 2D model
- Preliminary evaluation and development of a potential restoration alternative in conjunction with input from Tacoma Power (Appendix B)

# 4 Hydraulic Model Development

Anchor QEA was initially tasked with the development of a coarse-scale hydraulic model for the upper Cowlitz River and floodplain basin. The coarse-scale model was used to assess hydraulics of the system extending from the Cowlitz Falls Dam (Lake Scanewa) upstream to Packwood, Washington, and gain a better understanding of how the range of flows in the system change the channel and floodplain connectivity. To improve predictions of floodplain connectivity and informed detailed predictions of spatially varying depth-averaged velocity, the coarse-scale model was refined in the areas of the basin ranging from 3 miles downstream of Randle, Washington, to the upstream extent of the model near Packwood where channel thalweg bathymetry was available (see Section 4.3) and the river channel was largely unconfined. This refined model was then used to evaluate the detailed spatially varying hydraulics of the system over a range of flows from low-flow conditions up to the 10-year flood and estimate HSI values.

The following sections describe the development of the upper Cowlitz River basin coarse-scale and refined models (Sections 4.1 and 4.2), the development of the model boundary conditions (Section 4.5), the validation of the model predictions (Section 4.6), and the hydrodynamic simulations that were evaluated (Section 4.7). Report Sections 5 through 8 describe the application of the hydraulic results and their application for fisheries habitat suitability and preliminary evaluation of the model as a tool to assess and describe the outcome of potential restoration alternatives.

## 4.1 Coarse-Scale Model Development and Results

The U.S. Army Corps of Engineers (USACE) HEC-RAS version 5.0.5 was the modeling platform selected for the coarse-scale modeling evaluation (USACE 2016). The coarse-scale model was developed as a 1D model, using the upper Cowlitz River channel centerline and a total of 236 cross sections. The cross sections are spaced approximately every 400 to 800 feet along the river, to represent the river channel and floodplain elevations. The hydraulic predictive capabilities of the coarse-scale model were validated against LiDAR measurements of water surface elevation in the channel using a low-flow simulation and the results were also validated against the Federal Emergency Management Agency (FEMA) Flood Insurance Study (FIS) 100-year flood water surface elevation profile. The model was roughly calibrated based on a range of typical Manning's *n* roughness values. The model was then used to perform a series of preliminary hydrodynamic simulations that were used to evaluate the flow rates that cause flooding in the Cowlitz River, as well as how the hydraulics in the river channel change from low flow up to the 100-year flood event. These flooding and hydraulic condition results were used to help inform the most appropriate flows to simulate with the refined, finer-scale (detailed) model. Appendix A describes the development of the coarse-scale 1D hydrodynamic model and results.

## 4.2 Refined Model Framework

The USACE HEC-RAS version 5.0.5 was also used as the framework for the refined model. This refined model utilizes a combination of 1D and 2D modeling, with the lower extents of the model being composed of transects derived from the previously developed coarse-scale model, and the upper part of the model being composed of a new hydrodynamic mesh, consisting of computational grid cell polygons that define the geometry of the river and floodplain. The 2D and 1D sections of the model were hydraulically coupled during the dynamic simulations. Figure 4-1 shows the layout of the combined 1D/2D fine-scale model geometry as well as the general hydraulic areas of interest.

Sections 4.3 and 4.4 describe the development of the fine-scale model.

**Figure 4-1**
**Fine-Scale 2D Model Geometry**

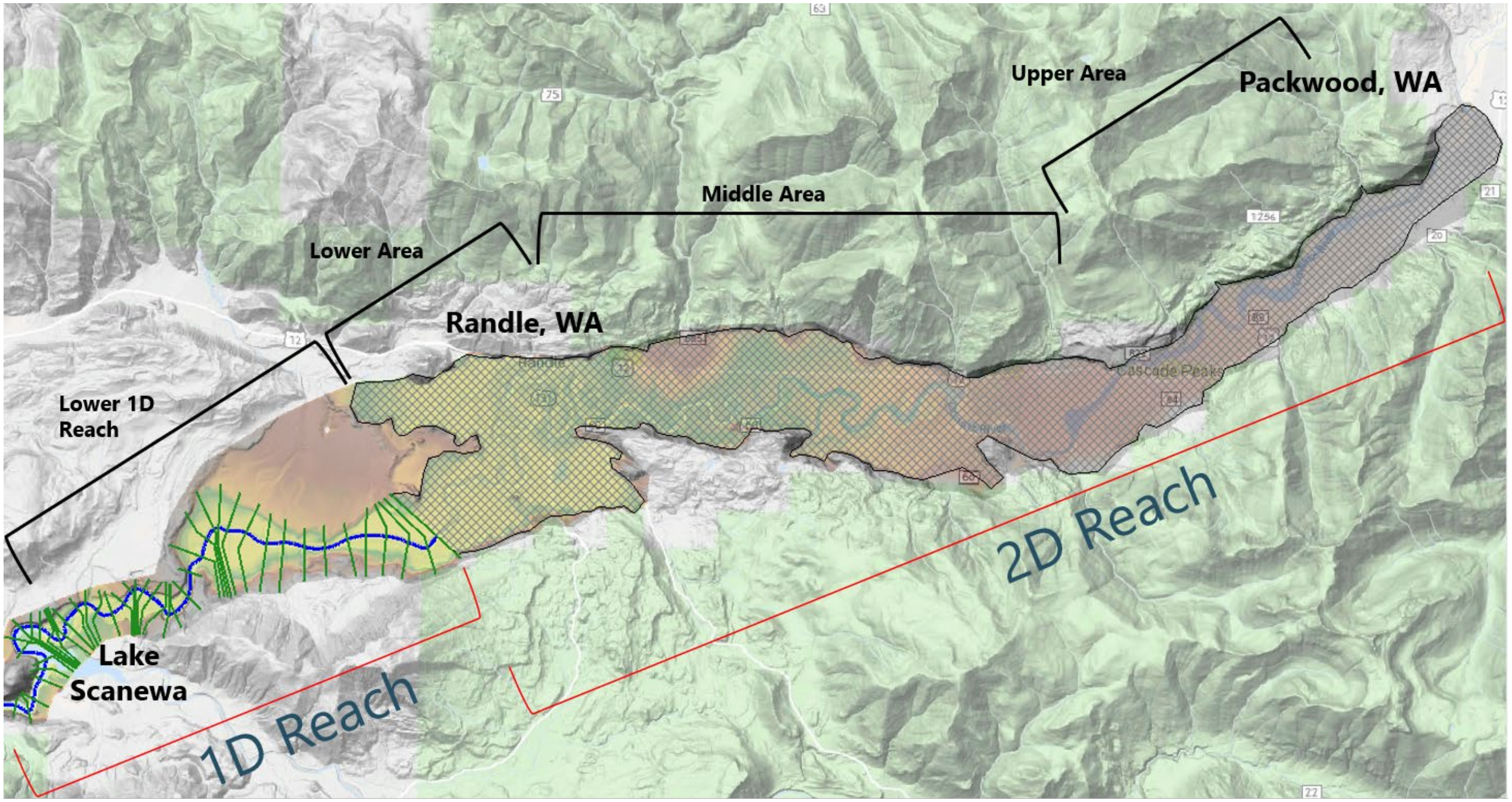

## 4.3 Model Topography and Bathymetry

The fine-scale 1D/2D model was developed using the site-wide topo-bathymetric aerial LiDAR survey data collected by Quantum Spatial, Inc. (QSI), in April 2018 (QSI 2018). The survey data extend from Cowlitz Falls Dam and Lake Scanewa upstream to approximately 2 miles south of Packwood, covering the entire width of the upper Cowlitz River basin. Figure 4-2 shows the extents of the LiDAR data coverage.

The survey employed a topo-bathymetric ("blue-green") type of LiDAR that was collected with an aerial based scanner on April 24 and 25, 2018, by QSI (2018) and provided to Anchor QEA as digital elevation surface for use as the channel and floodplain geometry of the hydraulic model. Data were provided in the North American Vertical Datum of 1988 (NAVD88) vertical datum, and this datum was used for the model geometry and water surface elevation prediction results. The survey data generally provided highly detailed (3- by 3-foot resolution) and complete coverage of the upper Cowlitz basin. The LiDAR was able to penetrate between 5 and 10 feet beneath the surface of the water in the channel and provide good data coverage for the upper (eastern) half of the LiDAR coverage where the water depth in the channel was shallower. In areas near Randle and downstream, water levels were deeper than the upper reaches and some data gaps were observed in the deepest pools of the channel where the LiDAR could not penetrate. Bathymetry data were not obtained for the lower areas of the upper Cowlitz, including the areas influenced by backwater from Lake Scanewa and extending all the way to the Cowlitz Falls Dam.

In order to develop riverbed elevations in the deeper water areas that were not captured by the LiDAR survey, an interpolation method was used to estimate elevations in the areas of missing data. Longitudinal profiles were interpolated between the upstream to downstream end of the missing data gaps in deep-water sections of the channel. The interpolated profile lines were then used to patch the areas of missing bathymetry by interpolating from either side of the riverbank where data were available. In the downstream backwater areas of Lake Scanewa, the channel thalweg profile from the 2006 FEMA FIS (FEMA 2006) for Lewis County was used to generate the channel bottom profile. The channel side-slope geometry was interpolated and used to patch the topo-bathymetric surface dataset. This interpolation in the downstream section of the 1D model area is not a concern for the accuracy of the hydraulic predictions upstream in the Randle, middle, and upstream hydraulic areas because the water levels at the downstream boundary are controlled by the Cowlitz Falls Dam (i.e., the river stage is not affected by the channel bathymetry in this area). Backwater influence from the reservoir has a minimal effect on water levels in the downstream sections of the 2D model. Therefore, the lack of detailed channel bathymetry in the downstream 1D sections of the model is not a concern for this modeling evaluation.

**Figure 4-2**
**Topo-Bathymetric Survey Extents**

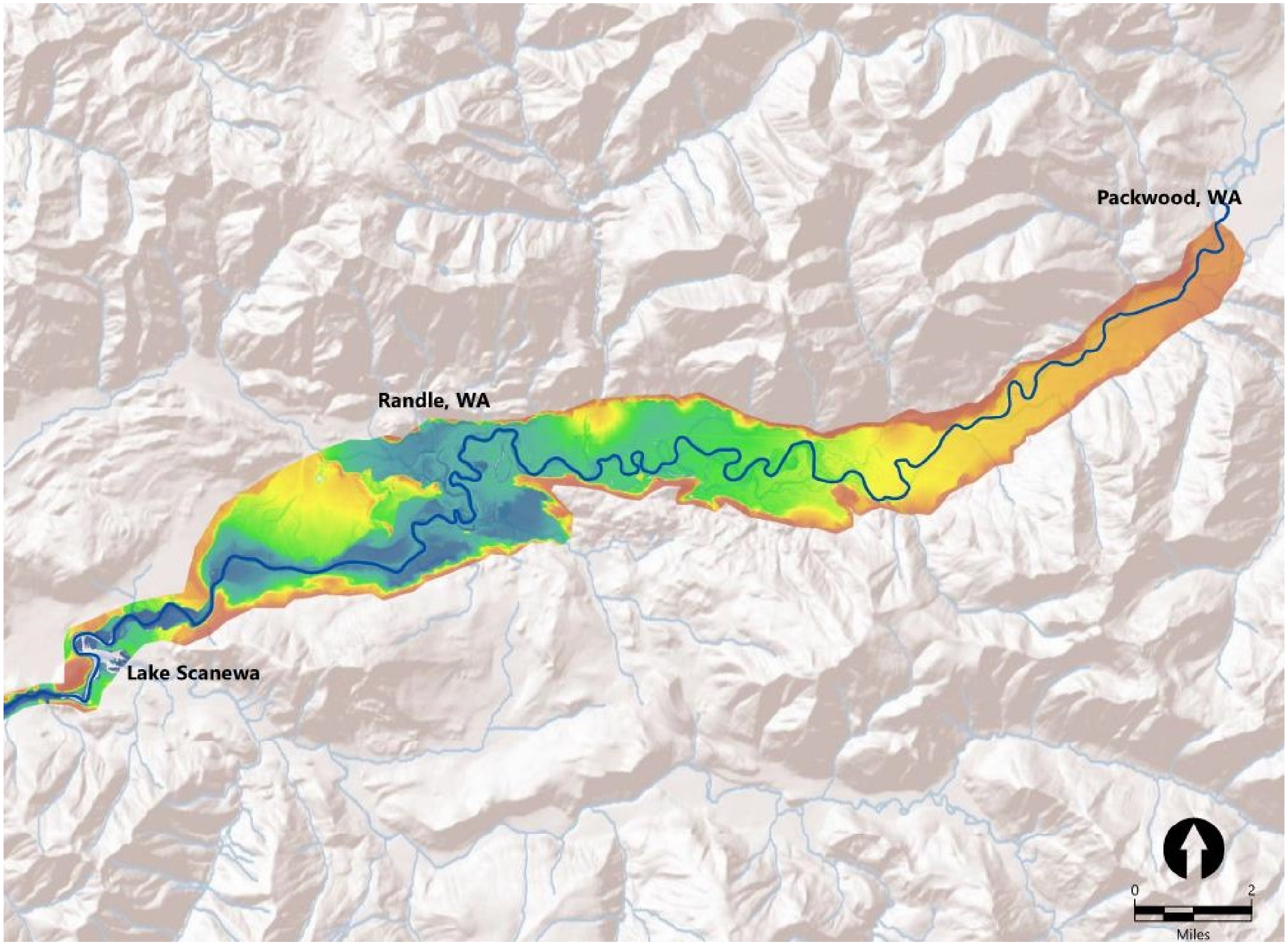

In addition to the deep-water areas in the channel and Lake Scanewa, there were a few small areas in the floodplain that may have had ponded water during the survey that did not have LiDAR elevations. While these small areas of missing data would have a non-measurable effect on the channel and floodplain hydraulics, the model requires complete coverage of terrain elevations. Therefore, these small areas were spatially interpolated across to provide a complete and continuous terrain surface for the floodplain of the 2D areas of the model.

The lower section of the fine-scale model that utilizes the 1D transects (Cowlitz Falls Dam to downstream of Randle) was left unchanged from the coarse-scale model described in Appendix A. For the 2D section of the model, the final LiDAR survey and patched terrain dataset was joined with the 2D (grid cell polygons, described in the following section) model grid to serve as the model geometry.

## 4.4 Model Grid

The 2D model grid was developed using the HEC-RAS RAS-Mapper spatial data software package. The upstream section of the model consists of a connected network of polygons that define the resolution of the hydraulic calculations, which are performed on a cell-by-cell basis. The 2D grid consists of 114,171 polygons ranging in size from 66 (approximately 8 feet by 8 feet) to 42,600 (approximately 210 feet by 210 feet) square feet. In the Cowlitz River channel and channel banks, as well as along roads or other potential barriers to flow in the floodplain, the resolution of the grid was constructed with higher resolution (smaller grid size) to provide more precise definition of these hydraulically important features. In areas where the terrain surface is flat, such as in the floodplain where hydraulics vary over a much larger scale, a much higher grid cell polygon size was used to increase model computational efficiency. Figures 4-3a and 4-3b show the grid cell resolution at two select areas of the grid, near Randle and near the upstream areas of the model closer to Packwood.

**Figure 4-3a**
**Typical 2D Model Grid Cell Resolution Used for Model**

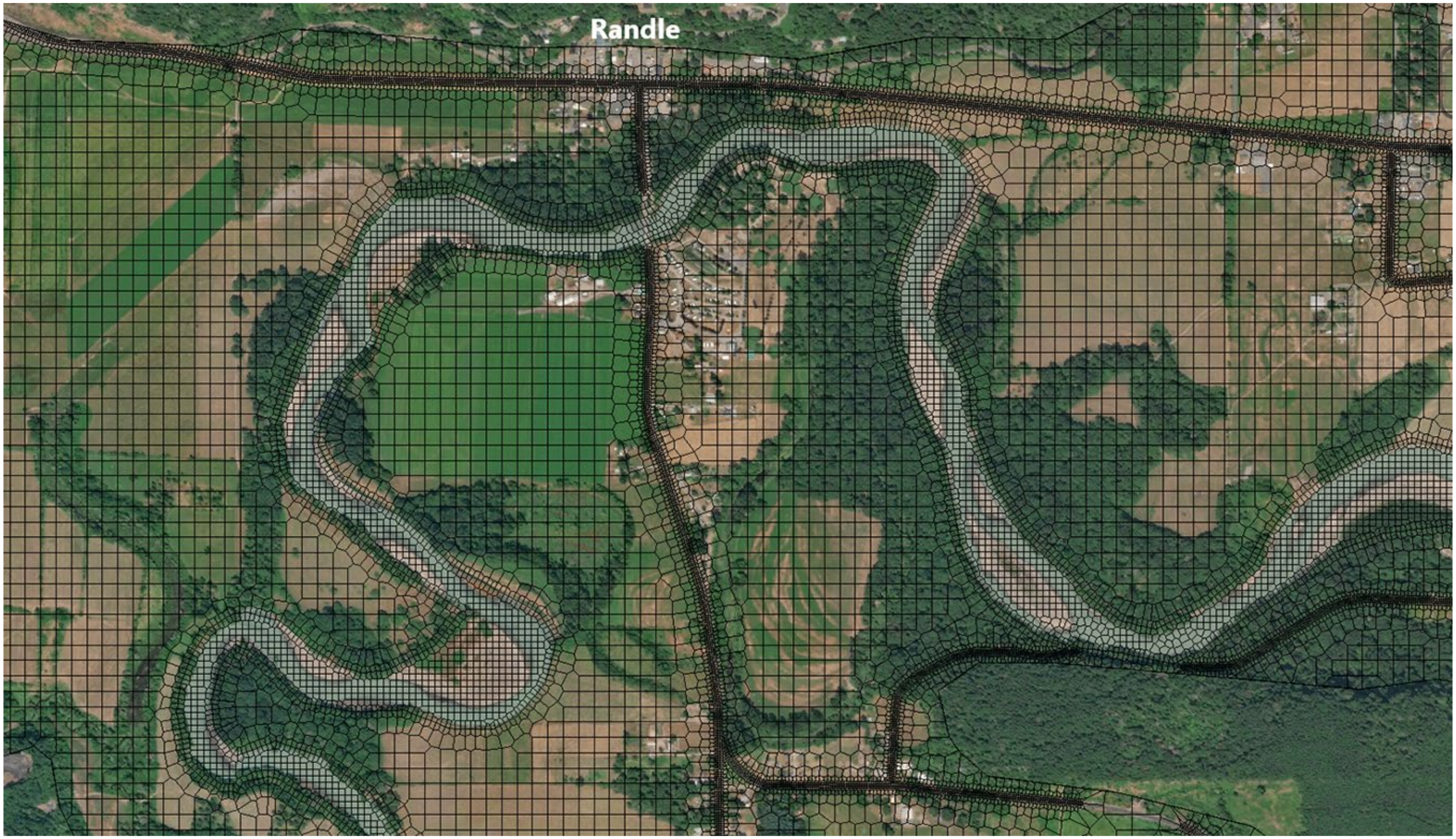

**Figure 4-3b**
**2D Model Grid Cell Resolution near Packwood**

## 4.5 Boundary Conditions

Boundary conditions for the model consisted of the flow rate inputs from the upper Cowlitz River and tributary inflows set at the Silver Creek confluence, water surface elevations in Lake Scanewa, internal boundary connection between the 2D and 1D model, and bed roughness. Figure 4-4 shows the location of the boundary conditions for the model. The 2D model results were computed and shown (Section 5) for the hatched areas. The 1D model results were not mapped as part of this evaluation because the focus of the floodplain connectivity and habitat evaluations was in the Randle, middle, and upstream hydraulic areas located upstream of the 1D section of the model.

The following sections describe the development of each boundary condition used in the hydrodynamic simulations.

### *4.5.1 Flow Rate Hydrology*

Two U.S. Geological Survey (USGS) gages are located within the 2D area of the model and were used to develop the flow rate boundary conditions for the model simulations. The first gage, USGS Gage No. 14226500 Cowlitz River at Packwood, Washington, was used for the primary upstream flow input boundary condition for the model. The second flow gage, USGS Gage No. 14231000 Cowlitz River at Randle, Washington, was used to estimate the flow increase between Packwood and Randle. Multiple named and unnamed tributaries join with the upper Cowlitz River between the Packwood and Randle gages. At the time of this study, point source flow inputs are not available within the HEC-RAS 2D modeling framework. This limitation makes it difficult to gradually increase flows in the main channel due to overland flow (i.e., runoff) and very small tributaries with channels that are not well defined by the LiDAR data.

The largest tributary between Packwood and Randle based on drainage area is Silver Creek, which is located approximately 3 river miles upstream from Randle (FEMA 2006). A flow input boundary condition for the Silver Creek tributary was used to provide a flow increase for the upper Cowlitz River main channel to account for the minor tributaries between Packwood and Randle (Section 4.7). While there was no available hydrology gage information for Silver Creek, the flow rate in Silver Creek was based on the flow difference between the Randle and Packwood gages for each model simulation. Because Silver Creek is the largest tributary based on drainage area, the lack of flow inputs from the other minor tributaries was not expected to significantly change the model results (Section 4.6). This is also supported by the evaluation of the flood hydrology at the two USGS gages for high flows, which suggests that the 10-year flood flow rate does not increase between Packwood and Randle. This suggests that the flow contributions to the main channel from tributaries and runoff during high flow events are small compared to likely snowpack melt occurring upstream of the Packwood gage. Adding each of the minor tributaries flow inputs to the model between Packwood and Randle would require a significant data collection effort (small streambed elevation surveys and flow rate monitoring) and model refinement at each junction with the river, and gains in model accuracy would be minimal at best. Therefore, the hydrology boundary conditions are as accurate as possible given the available information and current limitations of the modeling framework.

**Figure 4-4**
**Model Boundary Conditions and Hydrodynamic Areas**

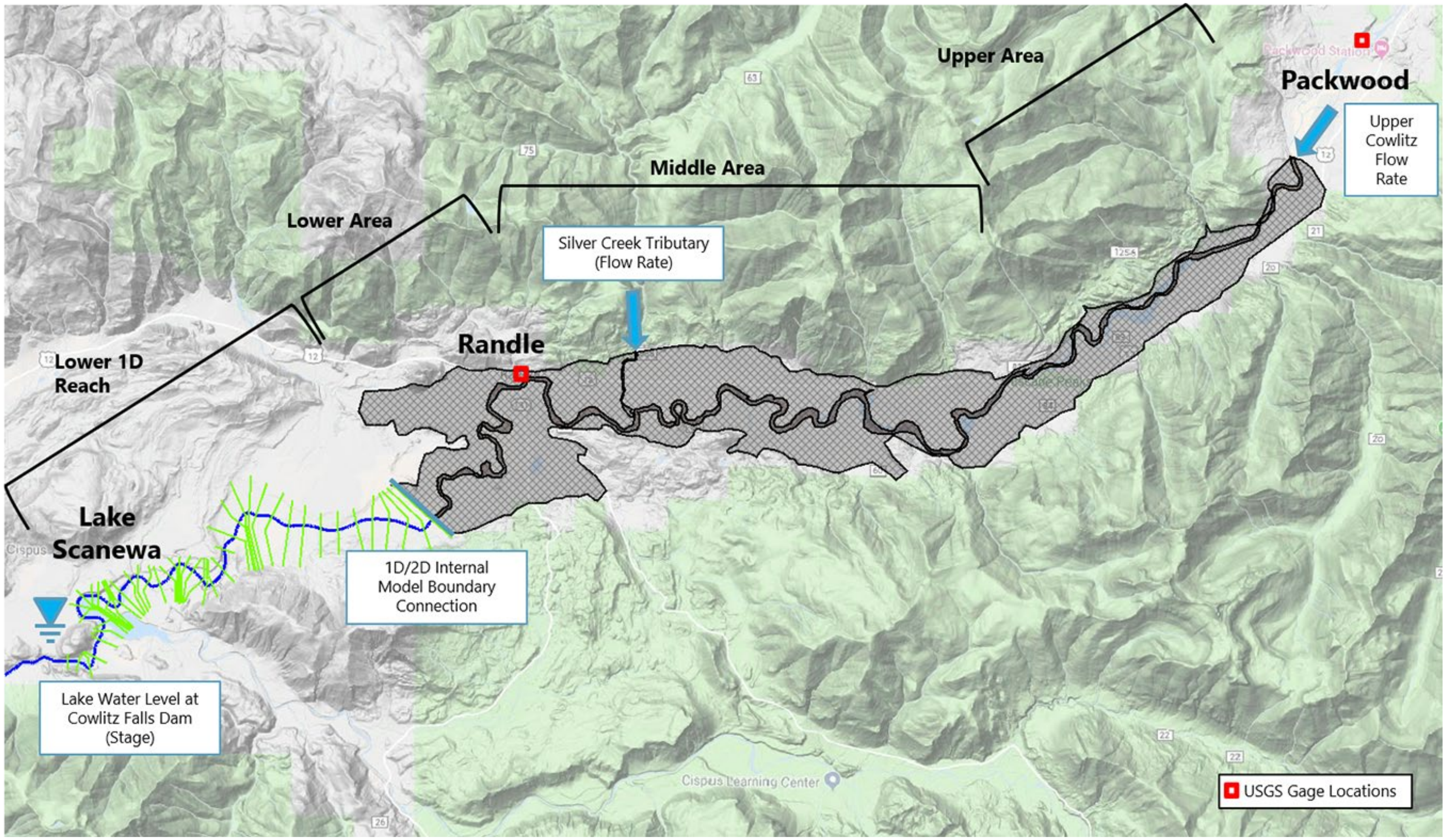

### 4.5.2 Lake Scanewa Water Levels

LCPUD maintains the water levels in Lake Scanewa per their operational license requirement. Water levels are maintained to optimize power generation depending on the flow rate in the river as well as to provide additional reservoir storage capacity during flood events. Table 4-1 summarizes the boundary condition regime that was used during the model simulations discussed in Section 4.7. The water surface elevation was applied to the lower 1D section of the model at the Cowlitz Falls Dam.

**Table 4-1**
**LC PUD Cowlitz Falls Dam Operation Conditions – Lake Scanewa Water Levels**

| Operational Condition | Upper Cowlitz Flow Rate[a] (cfs) | Lake Scanewa Water Level (NGVD29) | Lake Scanewa Water Level (NAVD88) |
|---|---|---|---|
| Low-flow conditions (no power generation) | 0–1,800 | 860–862 | 863.6–865.6 |
| Normal operations | 1,800–10,500 | 860–862 | 863.6–865.6 |
| Moderately high flow (operating) | 10,500–15,000[b] | 860 | 863.6 |
| Reservoir drawdown | 15,000[b]–27,000 | 846 | 849.6 |
| 100-year flood (all spillways open) | >90,000 | 846–852 | 849.6–855.6 |

Notes:

a. Flow rates are as measured at the USGS Kosmos gage No. 14233500 located at the Cowlitz Falls Dam unless noted otherwise.
b. Flow rate was measured at the USGS Randle No. 14231000 gage.

### 4.5.3 Internal 1D/2D Boundary

A hydraulic connection between the 2D (upstream) and 1D (downstream) sections of the model was established. The water surface elevation and flow rate predicted at the downstream boundary of the 2D model was established as the upstream boundary conditions for the 1D section of the model. The 1D hydraulic calculations were fully coupled and run simultaneously with the 2D calculations. The results from the coarse-scale model did not show any significant river restoration opportunities in the backwater-affected areas upstream of Lake Scanewa; therefore, using the 1D model to represent this reach resulted in increased computational efficiency.

### 4.5.4 Bed Roughness

Bed roughness was assigned to each hydrodynamic model grid cell polygon for the 2D section of the model and was spatially varied along the transects of the 1D section of the model. The bed roughness used in the HEC-RAS modeling platform is based on the Manning's *n* bed roughness coefficient. Two sources were used to provide Manning's *n* bed roughness coefficient values for the model grid. The off-channel and floodplain areas were assigned roughness coefficients using the publicly available USGS National Land Cover Database (NLCD; USGS 2016a) land use type values and applying typical roughness values for each land cover type based on published literature (Chow 1959; FEMA 2006). Values from the FEMA FIS for Lewis County were used in the upper Cowlitz River channel and Silver Creek tributary in-channel areas. Table 4-2 summarizes the Manning's *n* roughness values for all model simulations.

**Table 4-2**
**Manning's *n* Roughness Coefficient Values**

| Location | Manning's *n* Value | Source |
|---|---|---|
| Channel (Cowlitz) | 0.025 | FEMA 2006; Chow 1959 |
| Channel (Silver Creek) | 0.03 | FEMA 2006; Chow 1959 |
| Floodplain (agricultural) | 0.03–0.12 | USGS 2016a |
| Floodplain (dense vegetation) | 0.10–0.16 | USGS 2016a |

Note:
1. Values are the approximate range of values used. Floodplain varies in with NLCD land use type.

These values were revised in the area of the habitat restoration alternative assessment (Section 8) to appropriate values according to the proposed alternative actions.

## 4.6 Model Validation

Because calibration and validation gage data were not available for the scope of this modeling effort, a simple validation of the results for low-flow conditions was performed to ensure the model is accurately predicting flow within the channel banks prior to evaluating overtopping of the channel during higher-flow model simulations. The flow rates during the LiDAR survey measurements (April 24 and 25, 2018) were obtained from the Packwood and Randle USGS flow gages. The LiDAR dataset was a joined dataset of aerial surveys over these 2 days. The LiDAR provided rough estimates of the edge of water boundaries during the survey, which is an indicator of the approximate water surface elevation during the time of the survey. The average flow rate over the course of the 2-day survey was computed for each gage (1,520 cubic feet per second [cfs] for the Packwood gage and 2,987 cfs for the Randle gage), and the difference in the flow was used as the flow input boundary condition for the Silver Creek tributary (1,467 cfs). During these flow conditions, the model is expected to have some extra flows in the Silver Creek tributary to account for flows from minor tributaries located upstream. As described in Section 4.5.1, Silver Creek was the only tributary input into the model. The simulation was run in steady-state (constant flow rates and water levels) and the model-predicted water surface elevations, represented by the extents of the wetted perimeter in the channel, were compared to the measured boundary of the water in the channel from the LiDAR survey. Figure 4-5 shows an example of the validation comparison of the predicted wetted area (i.e., water surface elevation).

**Figure 4-5**
**Model Validation Simulation – Results Excerpt Between Randle and Packwood**

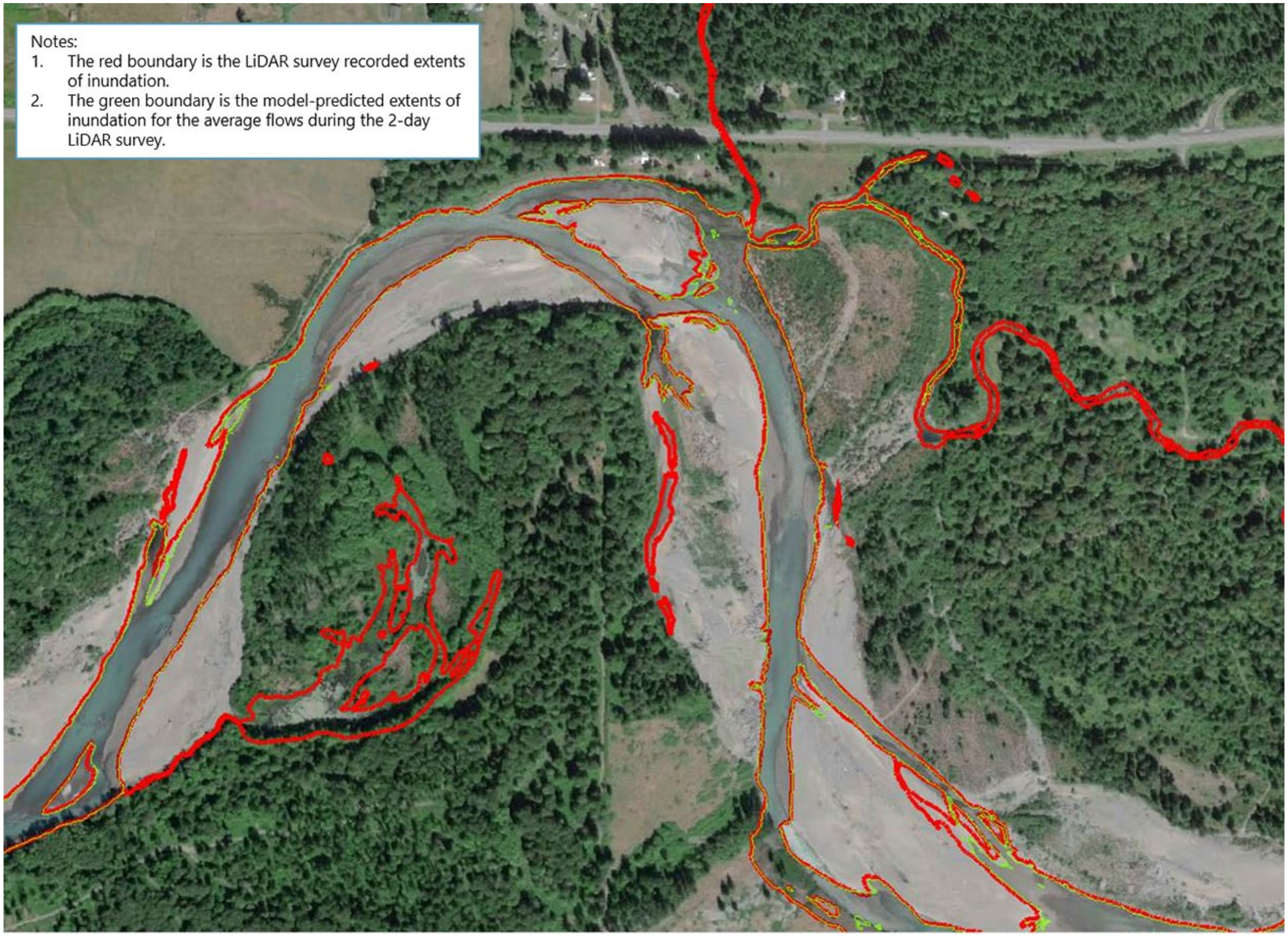

The predicted extents of flow in the channel show good agreement with the predicted water surface elevations in Figure 4-5 within 0.5 foot of the measured water surface elevation based on the LiDAR survey. There are multiple small-scale backwater channels and small ponded water areas that show up as red outlined areas that were not wetted during the model simulation due to the relatively coarse model grid cell resolution in this region of the model compared to the size of the small channels. The difference shown between the predicted inundation boundary and the boundary of water from the LiDAR survey in the off-channel areas could be occurring due to a number of factors such as the LiDAR not picking up micro-channel connections to backwater areas, the exact timing of the LiDAR survey vs. the flows used in the simulation from the flow record, or ponding due to rainfall showing up in the LiDAR survey that would not be predicted by the hydrodynamic model. Additional data were not available for calibration or validation during other flow conditions.

## 4.7 Hydraulic Simulations

The hydraulic simulations using the combined 1D/2D model were performed as dynamic simulations (time-varying boundary conditions). To simplify the number of simulations needed, the five different flow rates of interest were divided into two separate temporal simulations. Hydrographs of the two model simulations are presented in Figure 4-6 as well as the Lake Scanewa water surface elevations controlled by the Cowlitz Falls Dam used as the downstream boundary condition.

**Figure 4-6**
**Simulation Boundary Conditions**

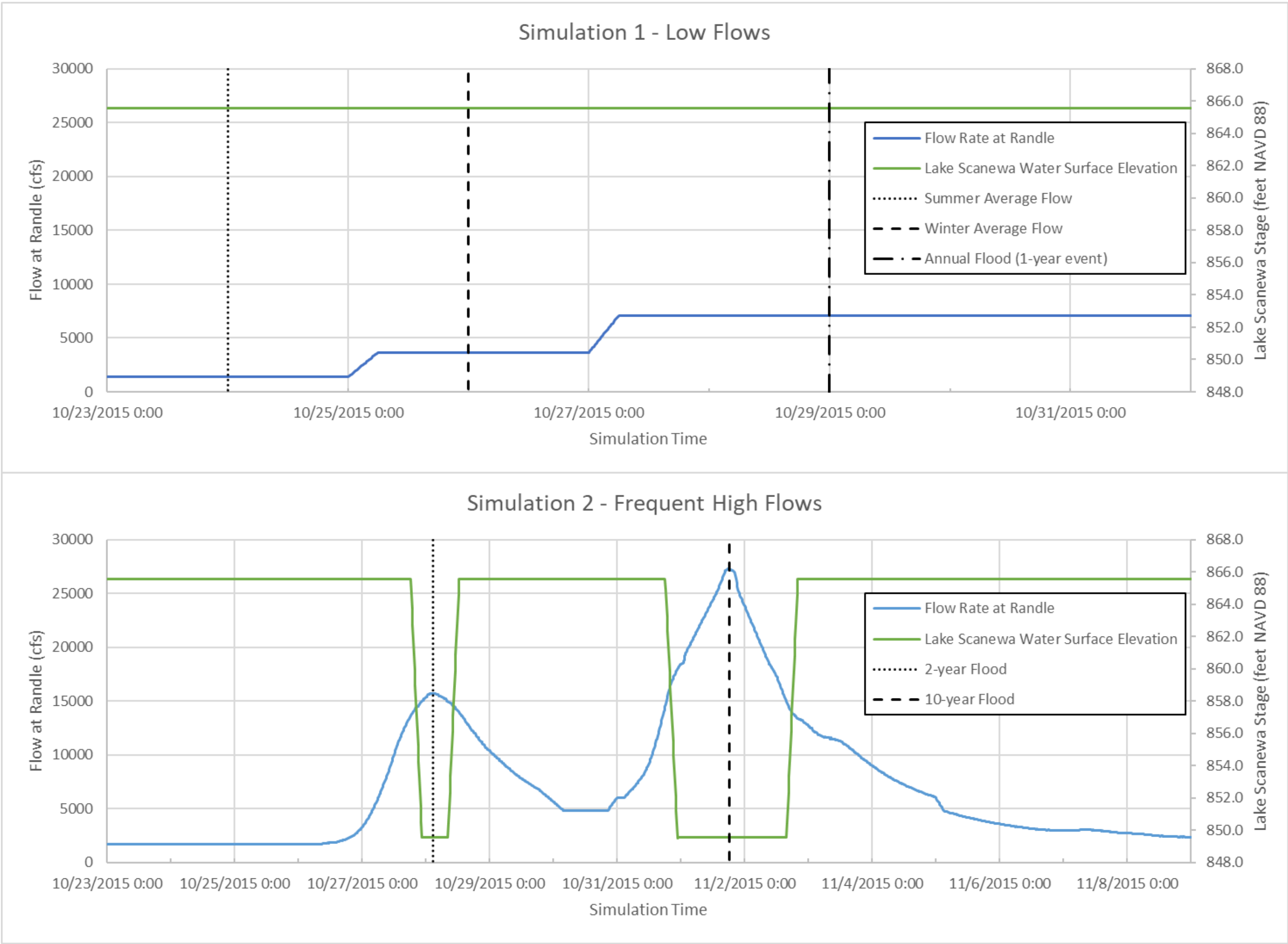

Simulation 1, low flows, included the summer average flow, winter average flow, and annual flood (i.e., the 1-year flood event). The summer average flow rate was computed as the mean daily flow rate for the 4 lowest flow months of July, August, September, and October. The winter average flow was computed as the average daily flow during the months of November through June when flows in the upper Cowlitz River are significantly higher. The annual flood (recurrence interval of 1 year) was computed using the PeakFQ toolset from USGS, as described in Section 4.5.1. Each of these flow rates for the first simulation were run in sequential order, from lowest to highest flow. The simulation started with the summer average low flow for the first 2 days of the simulation, at which point flows were gradually ramped up to the winter average flow over a 6-hour period and remained constant for approximately 40 hours. The flows were then ramped up again to the reach the 1-year flood level. During the entire simulation, the Lake Scanewa water levels remained constant because the flow rate was significantly less than the 15,000-cfs threshold requiring operational changes at the Cowlitz Falls Dam per the licensing requirements (Table 4-1).

Simulation 2, frequent high flows, included the 2-year and 10-year return interval event flow rates. These events were also run dynamically, with the peaks of each event occurring only for a short time, unlike the low-flow event simulation (Simulation 1), which ran a constant flow rate for approximately 40 hours for each flow of interest. The 2- and 10-year peak flood flows were the maximum flows in two separate flood waves (i.e., hydrograph peaks), which consisted of scaled versions of real flood events that were identified in the historical flow record. The peak of each of these floods was greater than the 15,000-cfs threshold for Cowlitz Falls Dam operational changes. When flows in the Cowlitz River at the USGS Randle gage exceeded 15,000 cfs, the water level in Lake Scanewa (water surface elevation boundary condition) was drawn down in the simulation over the course of 5 hours. Information concerning the rate of drawdown in the reservoir was not provided by LCPUD. After the peak of the 2-year hydrograph and 10-year hydrograph had passed, the water level in the LCPUD was again raised back to normal dam operational levels over the course of 5 hours. Results were evaluated for the peak of each flood event and were not evaluated during the periods of drawdown and filling of the reservoir; therefore, the rate of drawdown and filling was not critical information for this evaluation.

Table 4-3 summarizes the boundary conditions for each of the dynamic flow simulations and the subsequent evaluation that each flow rate scenario was used for.

**Table 4-3**
**Hydraulic Simulation Boundary Conditions and Application for Habitat Assessment**

| Dynamic Model Simulation | Flow Rate | Flow Rate at Packwood (cfs) | Flow Rate at Randle[1] (cfs) | Lake Scanewa Stage (feet NAVD88) | Results Evaluation |
|---|---|---|---|---|---|
| Simulation 1: Low flows | Summer average flow | 1,180 | 1,360 | 865.6 | HSI |
| | Winter average flow | 2,800 | 3,670 | 865.6 | HSI |
| | Annual flood event | 5,660 | 7,100 | 865.6 | HSI |
| Simulation 2: Frequent high flows | 2-year flood event | 15,000 | 16,200 | 849.6 | HSI, flood event hydraulics |
| | 10-year flood event | 27,300 | 28,500 | 849.6 | HSI, flooding evaluation |

Notes:

1. The flow rate at the Randle USGS gage No. 14231000 includes the flow from the Silver Creek tributary. Flows in Silver Creek were approximate baseline flows (non-flood event flow rates) for the frequent high-flow simulation and were based on the measured flow difference between the Randle and Packwood gages during low-flow conditions.
2. Lake Scanewa stage information was provided by Tacoma Power. See Section 4.5.2.

# 5 Hydraulic Results

The hydrodynamic model results for each evaluated flow rate (both Simulations 1 and 2) are provided as model results files and were plotted in a web map ([2D Model Web Map]). The results are shown on a small-scale view and presented from downstream (Lake Scanewa) and moving upstream to the upstream boundary of the model near Packwood. The results are broken down into reach scale views (which are referenced in the description of the results). The hydrodynamic parameters that are presented include depth-averaged velocity and water depth, which were mapped for the entire model grid. Warmer colors (yellow, orange, and red) are used to represent higher depth-averaged velocities (grid cell-averaged) and cooler colors (green and blue) are used to represent areas where depth-averaged velocity is low. For water depths, the color scales are the reverse, with shallow water areas mapped with warmer colors and deeper areas mapped with cooler colors. The hydraulic results are described in Sections 5.1 and 5.2.

## 5.1 Low-Flows Simulation Hydraulic Results

The low-flow simulation flow conditions (average summer flow, average winter flow, and annual flood flow) were used to represent the full range of typical hydraulic conditions occurring in the Cowlitz River on an annual basis. These hydraulic results (predicted depth-averaged velocity and depth) were exported from the modeling framework and the HSI composite values were computed (Section 6) based on these results for each flow rate.

The summer average flow (low flow) simulation results show that flows in each hydraulic area of the model (Randle to Packwood) are highly channelized and contained within the riverbanks. Figure 5-1 shows the predicted depth-averaged velocity at the upstream hydraulic area near Packwood. The flow generally follows one main flow path, with some islands. The aerial photography in this area shows where the primary channel has been historically and the large width of the extents of avulsion in this area. Spatially varying predictions of depth-averaged velocity in the channel range from 3 to 6 feet per second (fps) during summer average flows. Areas of the river basin near Randle show similar patterns, with highly channelized flow and no significant side channel or overbank connection opportunities. Maximum depth-averaged velocities in the lower basin were lower, between 1 and 2 fps with some areas up to 5 fps.

The winter average flows (average high flow) conditions simulation shows that flows are starting to fill the riverbanks, resulting in flow approaching "bank full" flow in the lower reaches near Randle and between Randle and Packwood below SR-12. Upstream near Packwood, the former channel alignments are not inundated, but some select side channels are starting to convey flow. Similar to the low-flow conditions simulation, there are no significant connections to floodplain storage during average winter flows. Figure 5-2 shows the water depth in the upper reach near Packwood (typically 5 to 10 feet) and the side channel south of the main channel beginning to activate and convey flow.

The annual flood simulation shows that flows have reached “bank full” conditions in the lower reaches of the model (river basin) as well as upstream near Packwood. In the lower reaches, there are some areas where numerous side channel and overbank storage areas (former channel avulsion areas) become inundated. In the upstream areas near Packwood, side channels begin to convey more significant flow volumes. Figure 5-3 shows the connection in middle valley area between Randle and Packwood where a backwater connection to a former avulsion channels has occurred.

Predicted depth-averaged velocities in the channel increase significantly for the annual flood, with velocities between 3 and 7 fps for the lower river basin reaches and up to 8 fps peak velocity near Packwood. Figure 5-4 shows the predicted depth-averaged velocity in the channel in the location of the lower basin where the former avulsion channel shows inundation. The predicted velocities in the main channel are between 3 and 7 fps while the velocities in the former avulsion channel are much lower, between 1 and 2 fps.

**Figure 5-1 Results Excerpt**
**Predicted Depth-Averaged Velocity near Packwood – Summer Average Flow**

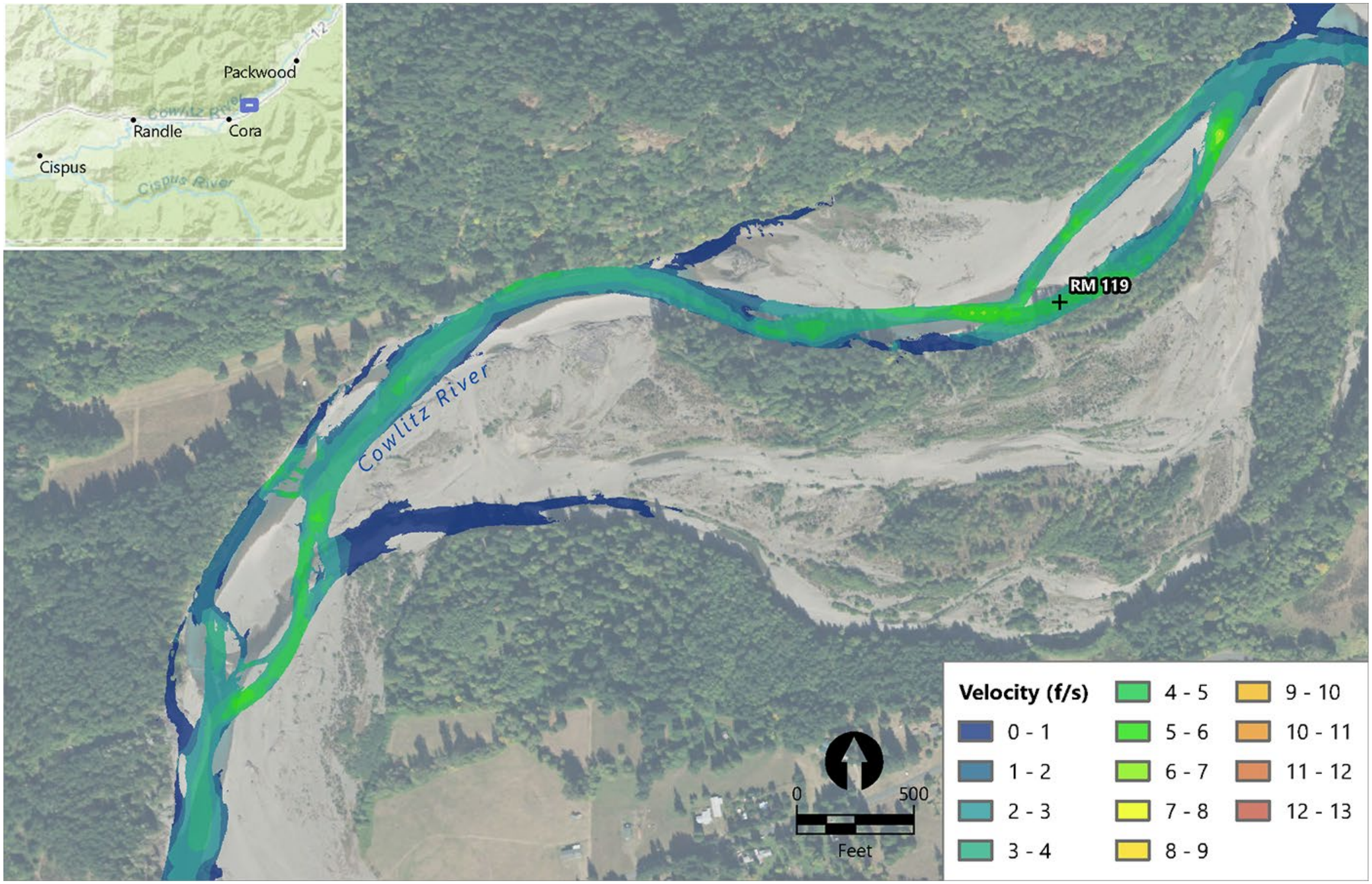

**Figure 5-2 Results Excerpt**
**Predicted Water Depth near Packwood – Winter Average Flow**

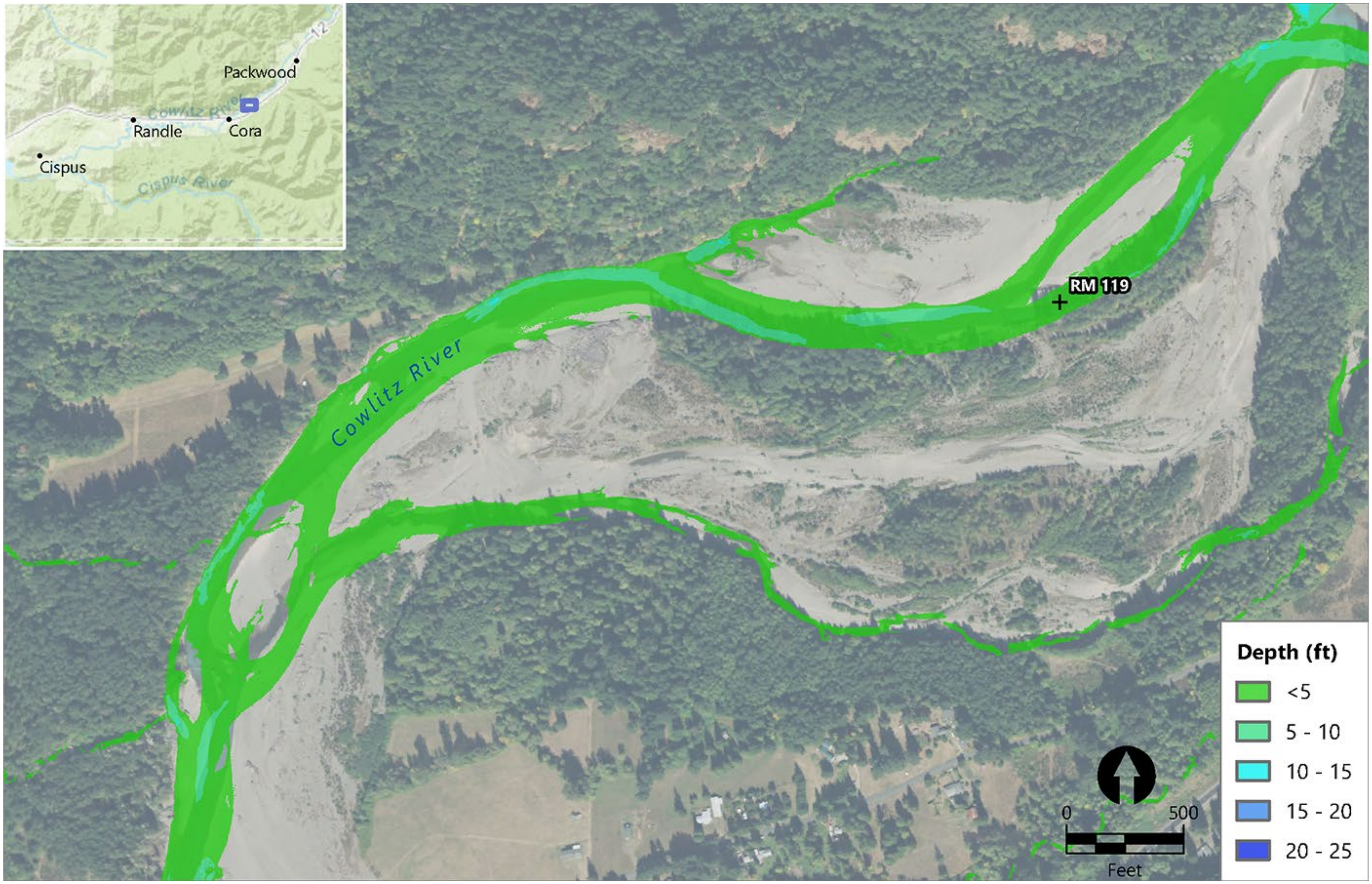

**Figure 5-3 Results Excerpt**
**Predicted Water Depth in the Middle Area Upstream of Randle – Annual Flood Event**

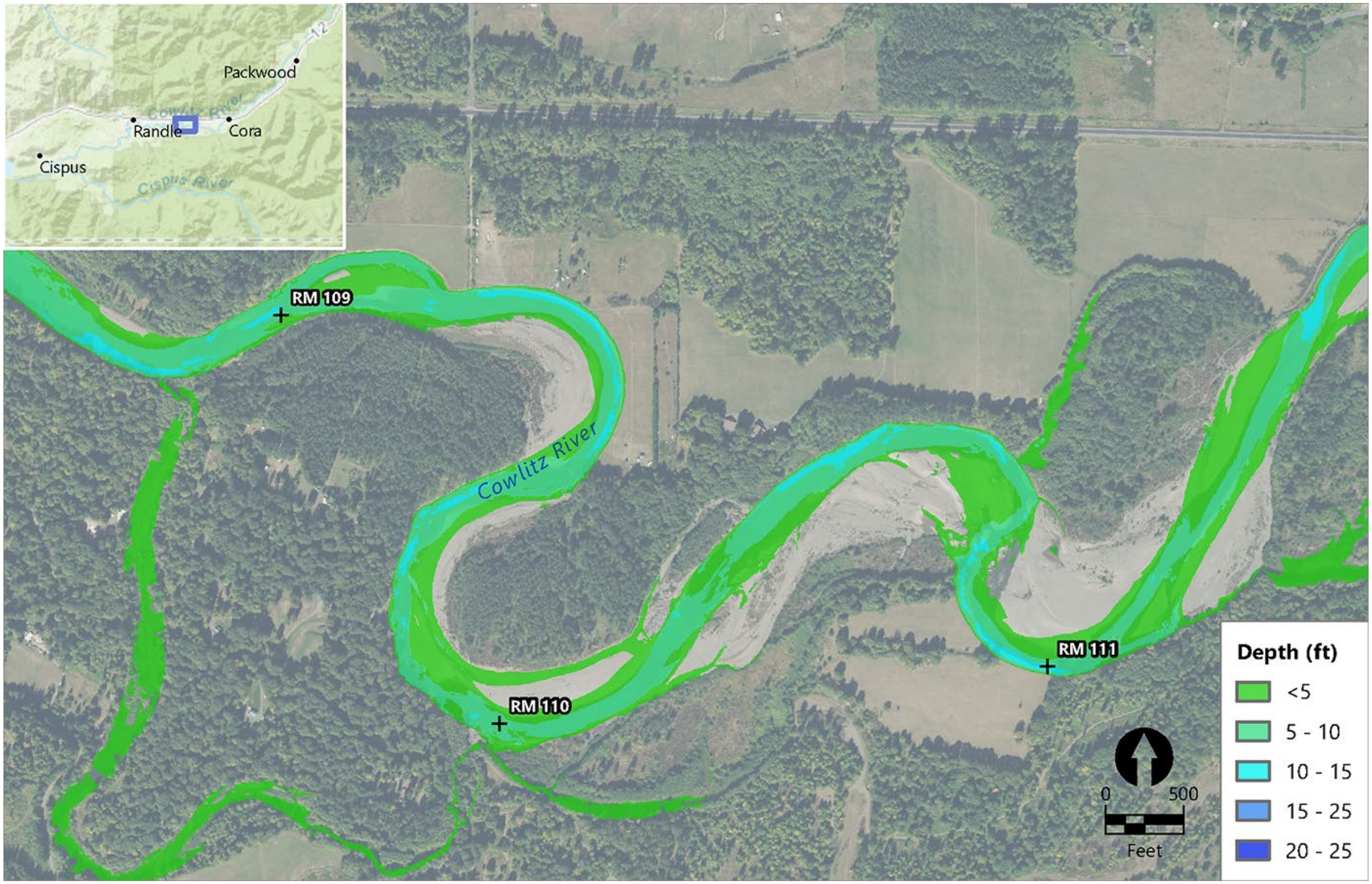

**Figure 5-4 Results Excerpt**

**Predicted Depth-Averaged Velocity in the Middle Area Upstream of Randle – Annual Flood Event**

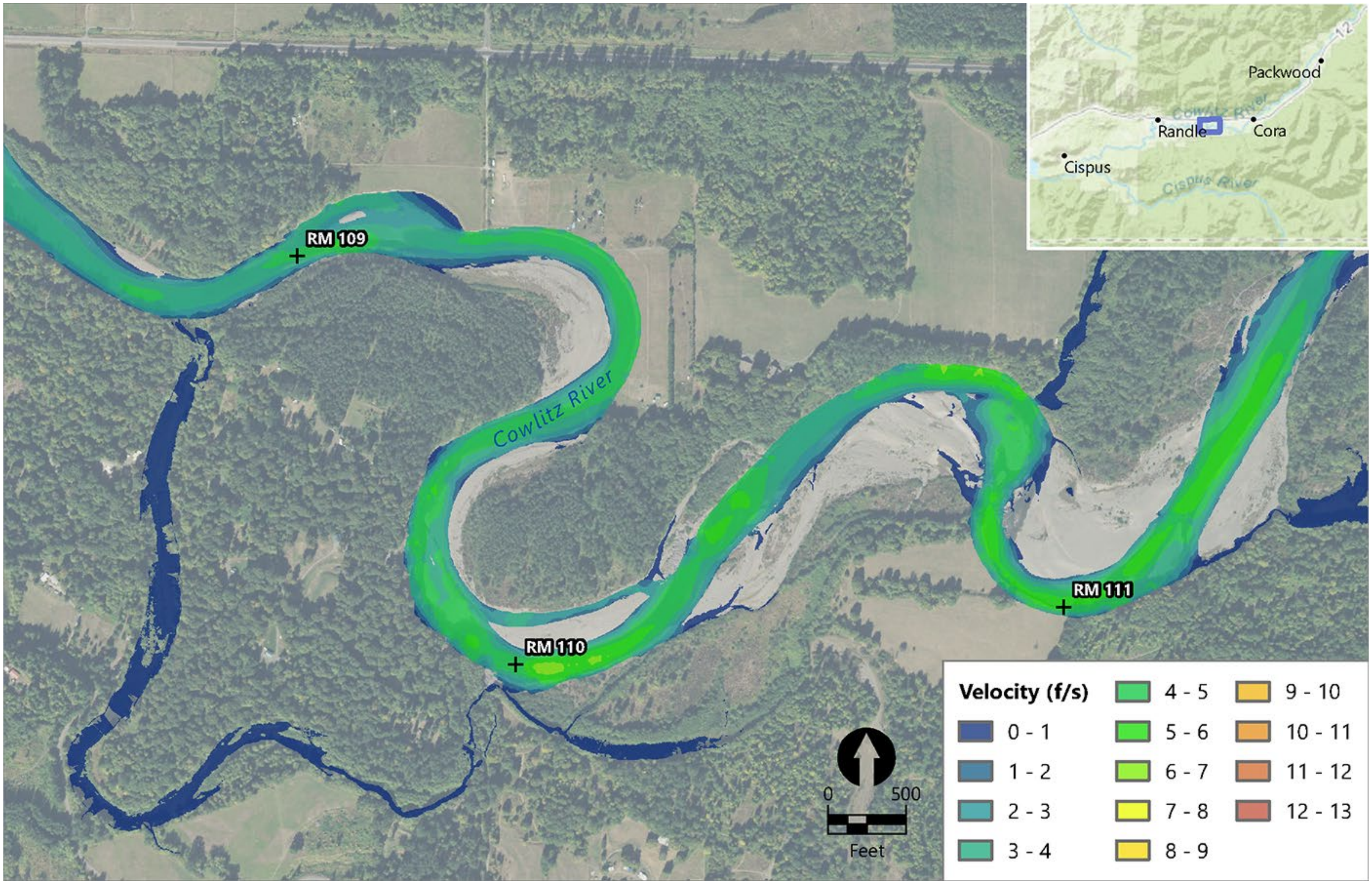

## 5.2 Frequent High-Flows Simulation Hydraulic Results

The 2-year flood hydraulics show flows overtopping the riverbanks and significant flows through the floodplain. The 2-year flood also shows significant connectivity with off-channel depressions (former channel avulsion locations) and side channels.

For the 2-year return interval flood event simulation, significant overtopping of the riverbanks and backwater side channel connectivity was predicted. Figure 5-5 shows the major overtopping of the riverbanks and backwatering (i.e., low velocity inundation connected at one location) of former avulsion channels near Randle, Washington. Depth-averaged velocities ranged from 3 to 8 fps in the channel.

Upstream near Packwood, Washington, the 2-year flood fills the former avulsion channels, which convey a significant amount of flow. Velocities in the channel ranges from 6 to 12 fps, and velocities in the former avulsion channels range from 1 to 4 fps. Figure 5-6 shows the width of the channel and avulsion channels near Packwood. There are also numerous smaller side channels that convey small amounts of flow during the 2-year flood event.

The 10-year flood represents a major flood event for this system. The hydraulic predictions for the 10-year flood were used to evaluate the extents of flooding in the Cowlitz River basin from downstream of Randle to Packwood. It is anticipated that these results will be used in the future to evaluate and support the potential targeted acquisitions in key areas in the upper basin for habitat restoration and flood mitigation measures. Figure 5-7 shows part of the extensive flooding in the river basin between Randle and Packwood near SR-12.

Predictions of high shear stress were also observed on the riverbanks during the 10-year flood simulation. The predicted shear stress during the peak of the 10-year flood is shown in Figure 5-8. Based on historical aerial photography in this area, the riverbank is rapidly eroding as the river channel shifts to the north. This erosional hotspot corresponds well with the predicted high shear stress.

**Figure 5-5 Results Excerpt**
**Predicted Depth-Averaged Velocity Near Randle, Washington – 2-Year Flood Event**

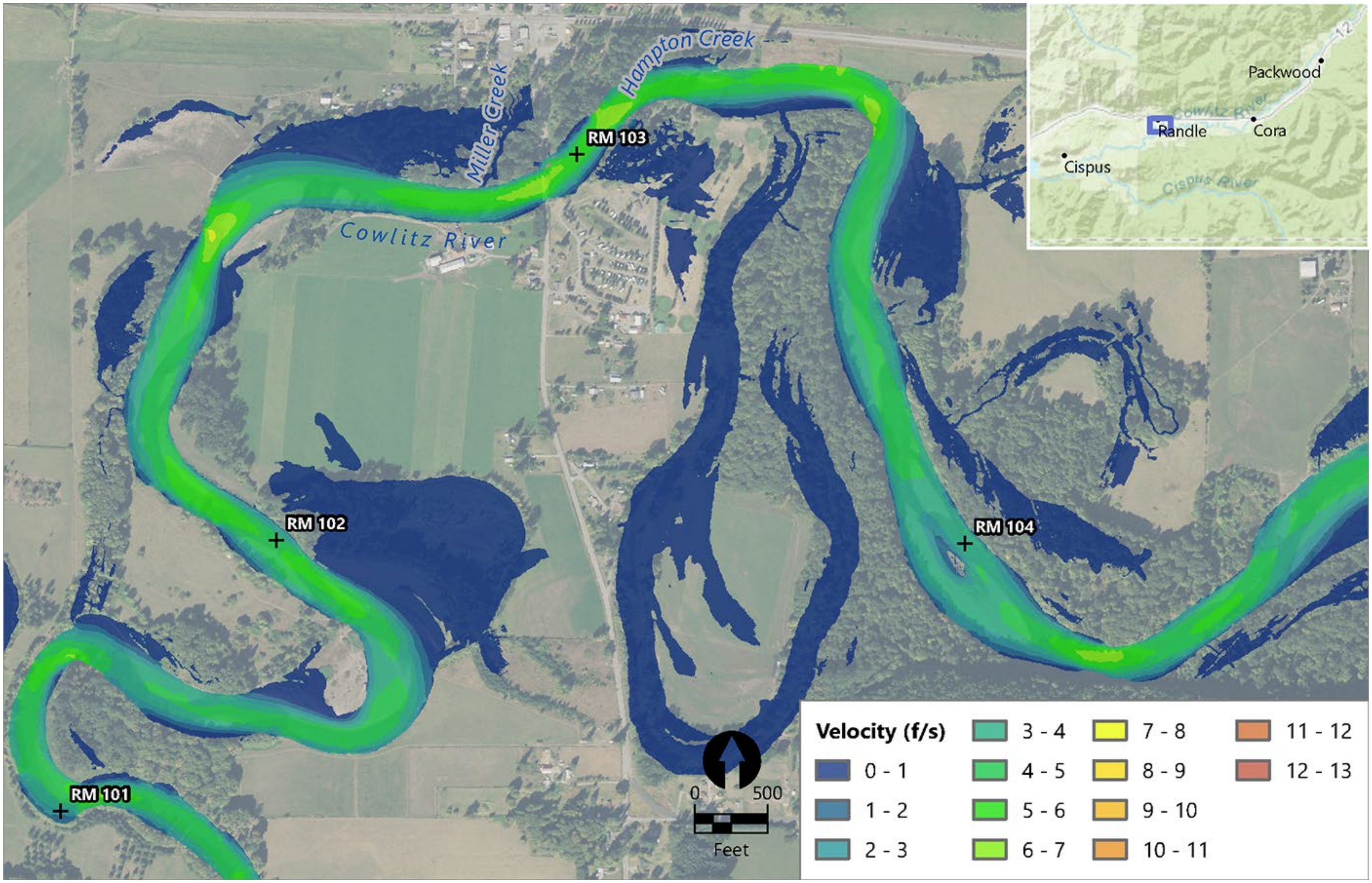

**Figure 5-6 Results Excerpt**
**Predicted Depth-Averaged Velocity near Packwood, Washington – 2-Year Flood Event**

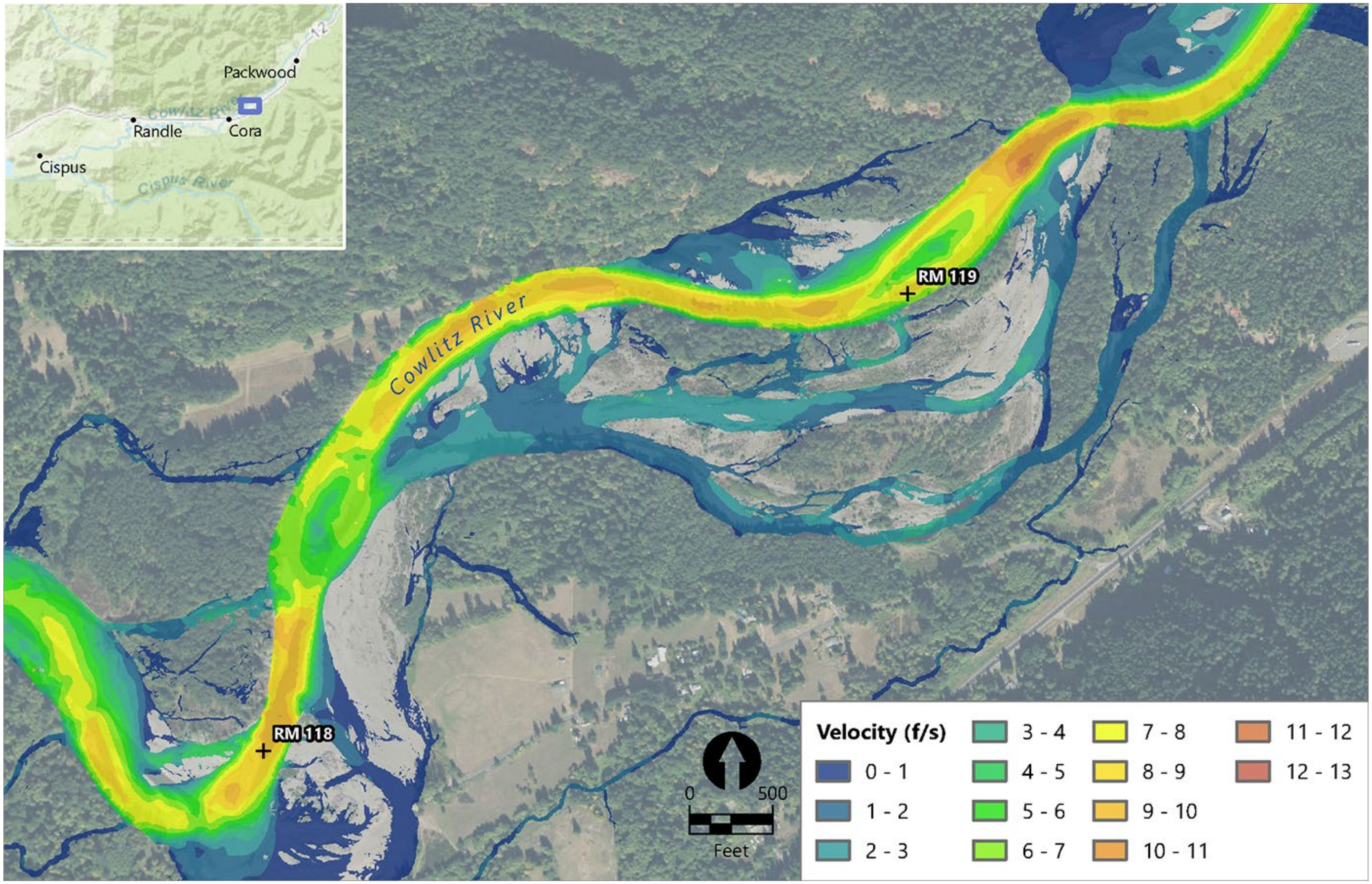

**Figure 5-7 Results Excerpt**
**Predicted Water Depth in the Upper River Basin – 10-Year Flood Event**

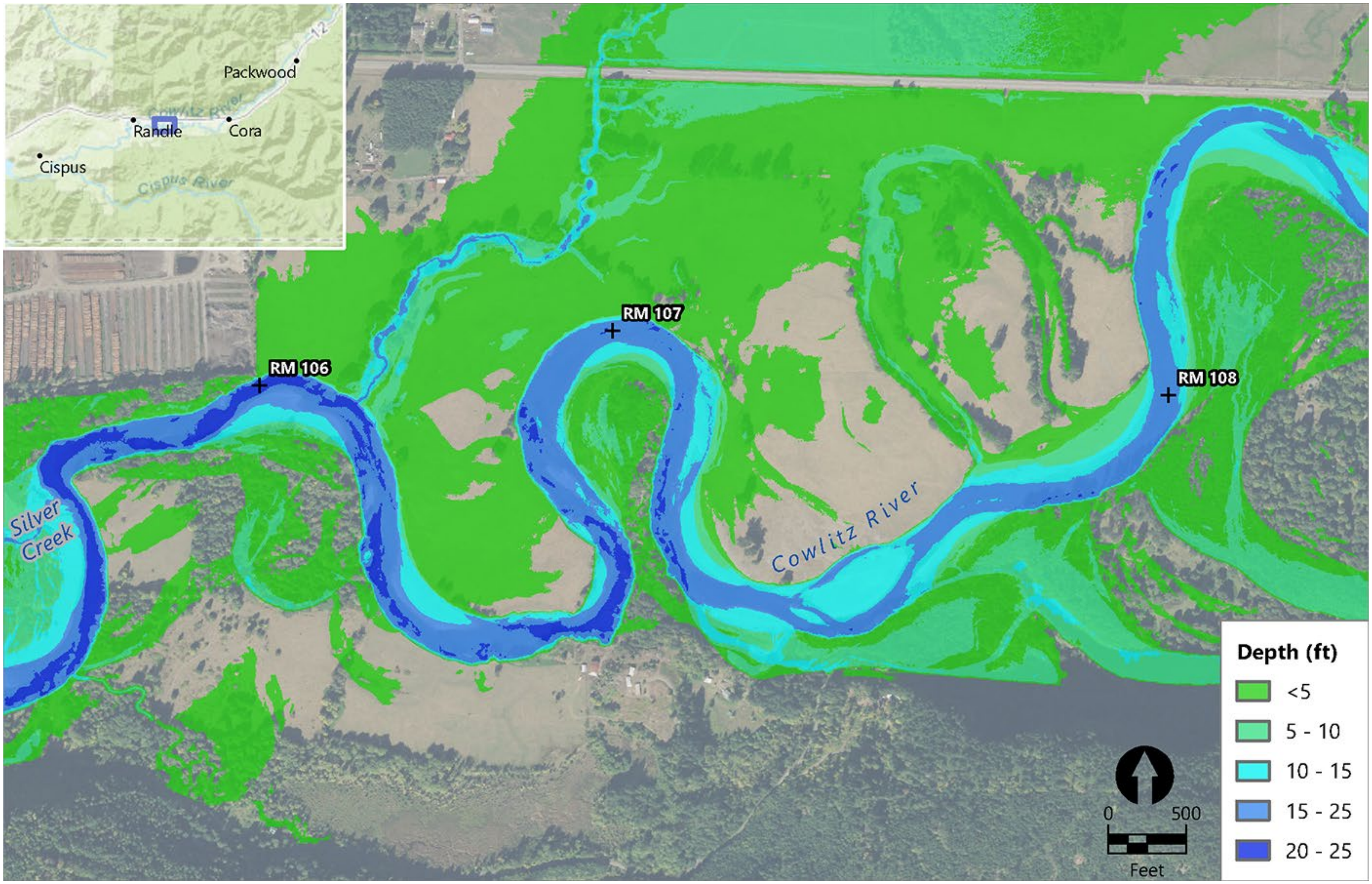

**Figure 5-8**
**Predicted Bed Shear Stress in the Upper River Basin – 10-Year Flood Event**

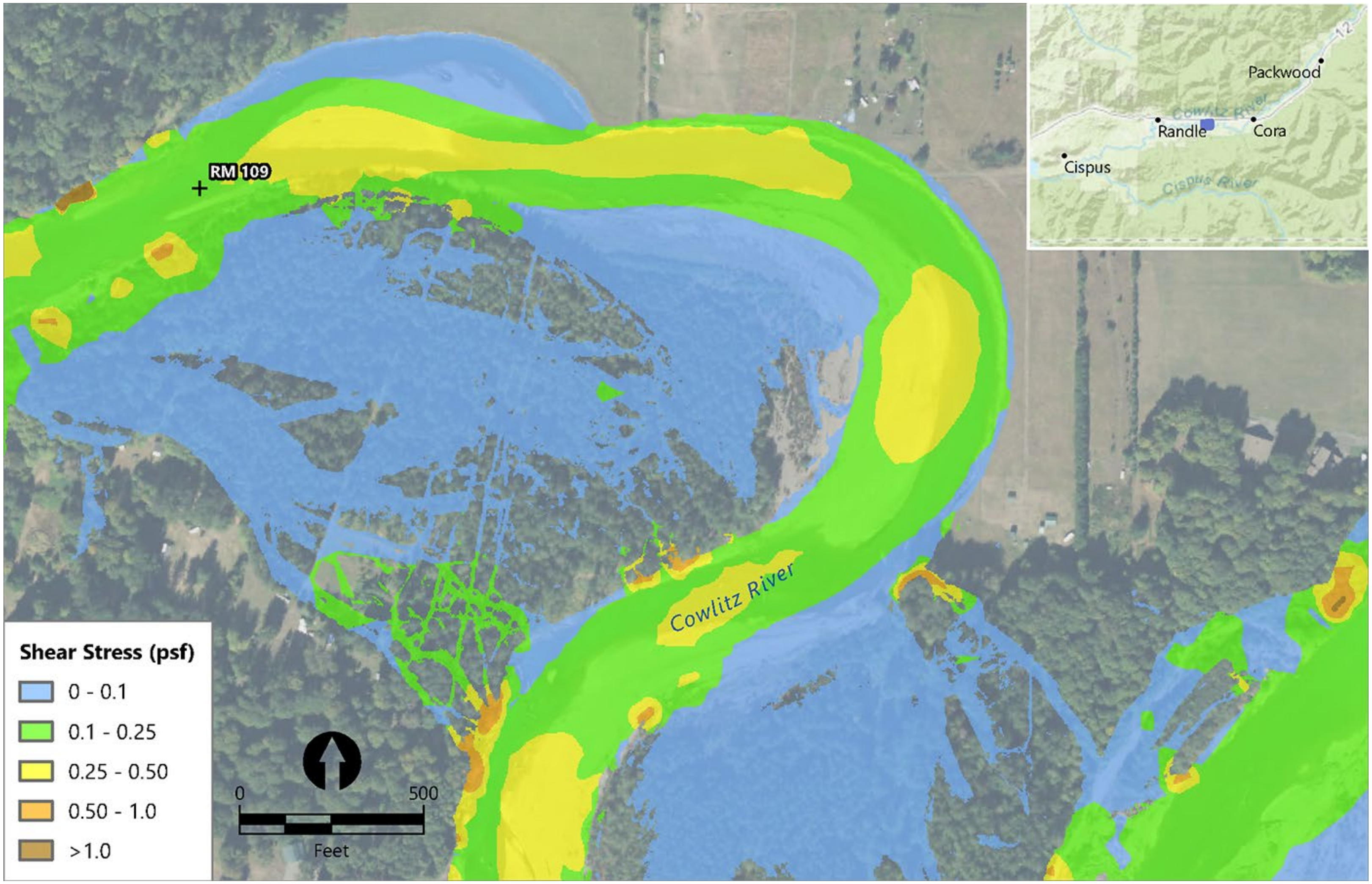

## 5.3 Hydraulic Results Summary

The following table provides a summary of how the hydraulics in the river change for each flow condition from both model simulations.

**Table 5-1**
**Summary of Hydraulic Results**

| Model Area | Area Length (River Miles) | Shallow Water Area (<0.5 foot) in Acres | | | | | High Velocity Area (>2.0 fps) in Acres | | | | |
|---|---|---|---|---|---|---|---|---|---|---|---|
| | | Summer Average Low Flow | Winter Average High Flow | Annual (1-Year) Flood | 2-Year Flood | 10-Year Flood | Summer Average Low Flow | Winter Average High Flow | Annual (1-Year) Flood | 2-Year Flood | 10-Year Flood |
| Lower Area (near Randle) | 5 | 13 | 7 | 11 | 92 | 156 | 51 | 178 | 232 | 267 | 316 |
| Middle Valley Area | 12 | 22 | 23 | 28 | 44 | 149 | 122 | 256 | 348 | 465 | 613 |
| Upper Area (near Packwood) | 7 | 19 | 23 | 27 | 43 | 75 | 108 | 162 | 209 | 335 | 439 |
| **Model Area** | **Area Length (River Miles)** | **Backwater Area (<0.5 fps) in Acres** | | | | | **High Shear Stress Area (>0.25 psf) in Acres** | | | | |
| | | **Summer Average Low Flow** | **Winter Average High Flow** | **Annual (1-Year) Flood** | **2-Year Flood** | **10-Year Flood** | **Summer Average Low Flow** | **Winter Average High Flow** | **Annual (1-Year) Flood** | **2-Year Flood** | **10-Year Flood** |
| Lower Area (near Randle) | 5 | 4 | 3 | 44 | 337 | 1180 | 3 | 10 | 14 | 20 | 75 |
| Middle Valley Area | 12 | 7 | 11 | 39 | 147 | 447 | 4 | 9 | 28 | 153 | 264 |
| Upper Area (near Packwood) | 7 | 10 | 17 | 20 | 31 | 53 | 15 | 48 | 126 | 271 | 384 |

Notes:

1. Backwater areas are connected areas to the main channel with limited flow through and low velocity (0.5 fps or less).
2. The threshold for high shear stress is based on the known threshold for coarse gravel movement from USGS established thresholds (USGS 2016b).

# 6 Habitat Suitability Index Evaluation

The HSI values for each section of the river were computed based on the predicted water depth and depth-averaged velocity model simulation results. For each flow rate condition, the HSI results were computed based on fish count observations for a wide range of hydraulic conditions with trendlines developed for each dataset. These HSI "curves" (i.e., HSI values as a function of predicted hydraulics) were then used to computed HSI values for both juvenile (1-year) Chinook and juvenile (1-year) steelhead salmonids based on the data published in *Instream Flow Study Guidelines: Technical and Habitat Suitability Issues Including Fish Preference Curves* (WDFW 2016). Initially, one HSI value based on depth-averaged velocity and one HSI value based on predicted water depth were computed from each HSI curve for each species. These HSI values were then multiplied together to obtain a composite representative HSI value with predicted depth-averaged velocity and water depth being weighted equally. After evaluation of these computed composite HSI values, the evaluation was refined using modifications to the published HSI curves based on experience with other similar river systems and information obtained through personal communication with Eric Beamer (Skagit River System Cooperative) in November 2018 related to state of the science HSI application. The modifications made by Anchor QEA were used to simplify the HSI values based on depth and areas with low predicted depth-averaged velocity and provide more representative HSI values for the Cowlitz River system. The published HSI curves for velocity and depth modified for this evaluation, for each species of interest, is summarized in Table 6-1 (juvenile Chinook salmon) and Table 6-2 (juvenile steelhead).

**Table 6-1**
**Juvenile Chinook Salmon Depth and Velocity HSI Preference Thresholds**

<table>
<tr><th colspan="3">Velocity</th><th colspan="3">Depth</th></tr>
<tr><th>Predicted Depth-Averaged Velocity Thresholds (fps)</th><th>HSI Value (WDFW)</th><th>HSI Adjusted Value[1] (Anchor QEA)</th><th>Predicted Water Depth Thresholds (feet)</th><th>HSI Value (WDFW)</th><th>HSI Adjusted Value[2] (Anchor QEA)</th></tr>
<tr><td>0</td><td>0.24</td><td rowspan="5">1.00</td><td>0</td><td>0.00</td><td>0.00</td></tr>
<tr><td>0.15</td><td>0.30</td><td>0.45</td><td>0.00</td><td>0.00</td></tr>
<tr><td>0.55</td><td>0.85</td><td>0.5</td><td></td><td rowspan="6">1.00</td></tr>
<tr><td>0.95</td><td rowspan="2">1.00</td><td>1.05</td><td>0.30</td></tr>
<tr><td>1.05</td><td>1.65</td><td>0.85</td></tr>
<tr><td>1.85</td><td>0.45</td><td>0.45</td><td>2.05</td><td>0.95</td></tr>
<tr><td>3.65</td><td rowspan="2">0.00</td><td rowspan="2">0.00</td><td>2.45</td><td>1.0</td></tr>
<tr><td>99</td><td>99</td><td>1.0</td></tr>
</table>

Notes:
Grey-shaded cells indicate no value for the listed threshold.
HSI values for hydraulic results that fall in between the listed threshold values were linearly interpolated, except for the depth HSI, which is binary 0 or 1.0 HSI value based on the 0.5-foot water depth threshold value.

1. The velocity HSI value modifications were based on the assumption that the backwater areas of the upper Cowlitz River basin with sufficient depth, but low velocities, would be suitable temporary habitat during higher-flow events but may not be suitable long-term habitat due to stagnation. Therefore, the low velocity HSI values were increased to 1.0 compared to the reported values. These areas of low velocity are shown in the HSI results web maps.
2. The depth HSI value curve was simplified to a binary value, where predicted depth greater than or equal to 0.5 foot was given a high suitability value of 1.0 and areas with less than 0.5 foot of water depth were considered not suitable habitat (HSI value of 0.0).

**Table 6-2**
**Juvenile Steelhead Depth and Velocity HSI Preference Thresholds**

<table>
<tr><th colspan="3">Velocity</th><th colspan="3">Depth</th></tr>
<tr><th>Predicted Depth-Averaged Velocity Thresholds (fps)</th><th>HSI Value (WDFW)</th><th>HSI Adjusted Value[1] (Anchor QEA)</th><th>Predicted Water Depth Thresholds (feet)</th><th>HSI Value (WDFW)</th><th>HSI Adjusted Value[2] (Anchor QEA)</th></tr>
<tr><td>0</td><td>0.55</td><td rowspan="3">1.00</td><td>0</td><td>0.00</td><td>0.00</td></tr>
<tr><td>0.75</td><td rowspan="2">1.00</td><td>0.15</td><td>0.00</td><td>0.00</td></tr>
<tr><td>0.95</td><td>0.50</td><td></td><td rowspan="5">1.00</td></tr>
<tr><td>1.15</td><td>0.87</td><td>0.87</td><td>0.65</td><td>0.30</td></tr>
<tr><td>1.55</td><td>0.78</td><td>0.78</td><td>1.35</td><td>0.85</td></tr>
<tr><td>1.85</td><td>0.54</td><td>0.54</td><td>2.65</td><td>0.95</td></tr>
<tr><td>3.15</td><td>0.30</td><td>0.30</td><td>99</td><td>1.00</td></tr>
<tr><td>3.85</td><td>0.07</td><td>0.07</td><td colspan="3" rowspan="3"></td></tr>
<tr><td>5</td><td rowspan="2">0.00</td><td rowspan="2">0.00</td></tr>
<tr><td>99</td></tr>
</table>

Notes:
Grey-shaded cells indicate no value for the listed threshold.
HSI values for hydraulic results that fall in between the listed threshold values were linearly interpolated, except for the depth HSI which is binary 0 or 1.0 HSI value based on the 0.5-foot water depth threshold value.

1. The velocity HSI value modifications were based on the assumption that the backwater areas of the upper Cowlitz River basin with sufficient depth, but low velocities, would be suitable temporary habitat during higher-flow events such as many of the events evaluated, but may not be suitable long-term habitat due to stagnation. Therefore, the low-velocity HSI values were increased to 1.0 compared to the reported values. These areas of low velocity were noted on the HSI results figures in Attachment 2.
2. The depth HSI value curve was simplified to a binary value, where predicted depth greater than or equal to 0.5 foot was given a high suitability value of 1.0 and areas with less than 0.5 foot of water depth were considered not suitable habitat (HSI value of 0.0).

The numerical HSI values were binned into three groups for low, moderate, and high composite (i.e., based on predicted depth-averaged velocity and water depth) HSI values. Table 6-3 shows the bin classifications (low, moderate, and high suitability metrics). In addition, areas where the water depth has high suitability, but the depth-averaged velocity is low, are shown as hatched areas. These areas are largely backwater areas that may be suitable temporary habitat based on the water depth but the quality of habitat could be improved if a flow connection was made in these areas to increase flow through velocity. Areas where the predicted water depth is too shallow and causes a reduction in the composite HSI values are shown as purple areas.

**Table 6-3**
**HSI Results Categories**

| Composite HSI Range | Suitability Rating | HSI Results Color Scale |
|---|---|---|
| 0.00–0.33 | Low | Red |
| 0.34–0.66 | Moderate | Yellow |
| 0.67–1.00 | High | Blue |

Note:
1. The HSI values for depth-averaged velocity and water depth were multiplied together to form composite HSI values.

## 6.1 Low-Flow Simulation HSI Results

There was limited hydraulic connection between the channel and overbank or side channel areas for the summer average flow and winter average high-flow conditions over the entire area of interest in the model (Randle, middle area, and upstream area near Packwood). Areas of high habitat suitability were generally limited to areas near the riverbanks or backwater areas within the channel near sandbar islands where predicted velocities area low (1 to 2 fps) and water depths were predicted to be greater than 0.5 foot.

For the annual flood event simulation, the computed HSI results were improved in backwater overbank areas that started to connect to the main channel. Figure 6-1 shows the limited areas of high suitability (blue areas) for the winter average flow conditions in the upper river basin above Randle for juvenile Chinook salmon. The hatched areas show areas of backwater flow where predicted depth-averaged velocities are below 0.25 fps. Purple areas show locations where water depth is too shallow for suitable habitat based on the HSI thresholds provided in above Tables 6-1 and 6-2. The hatched backwater areas tend to coincide with areas of good habitat suitability (blue shading).

**Figure 6-1**
**Predicted HSI Results in the Upper River Basin – Annual Flood Event – Juvenile Chinook Salmon**

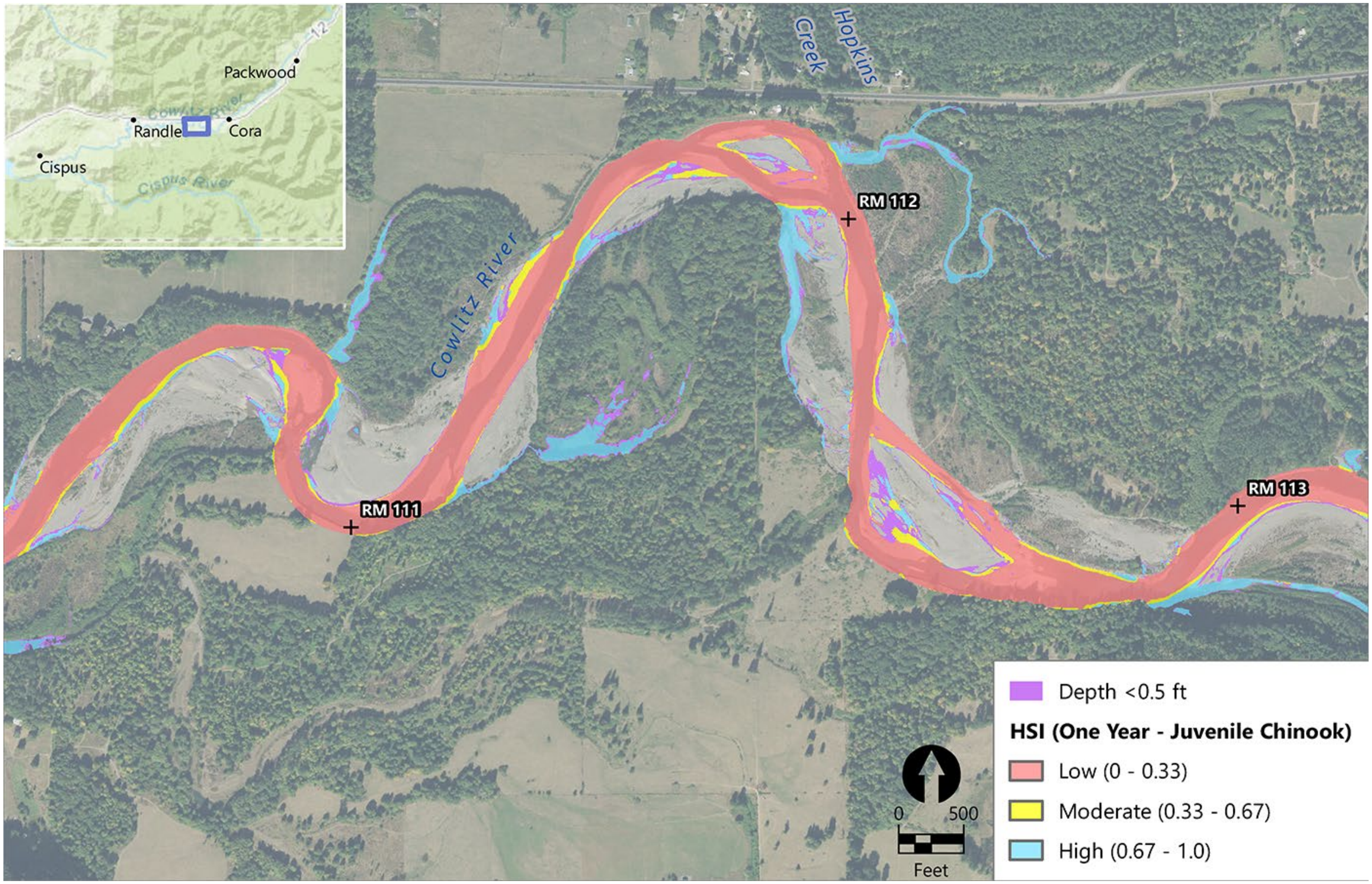

## 6.2 Frequent High-Flow Simulation HSI Results

The 2-year flood event showed good connectivity to overbank former avulsion channels and showed large areas of suitable habitat. Figure 6-2 shows the HSI results for the 2-year flood event for juvenile Chinook salmon, and Figure 6-3 shows HSI results for juvenile steelhead in the upper river basin between Randle and Packwood.

In the upper extent of the model near Packwood, there are numerous side channels with moderate to good habitat suitability; however, there are no large backwater areas in former avulsion channel locations. High predicted depth-averaged velocities in the upper reaches near Packwood result in reduced habitat suitability in the side channels compared to the backwater areas in the lower basin.

The 10-year flood event simulation was not evaluated for habitat suitability due to its infrequent occurrence.

**Figure 6-2**
**Predicted HSI Results in the Upper River Basin – 2-Year Flood Event – Juvenile Chinook Salmon**

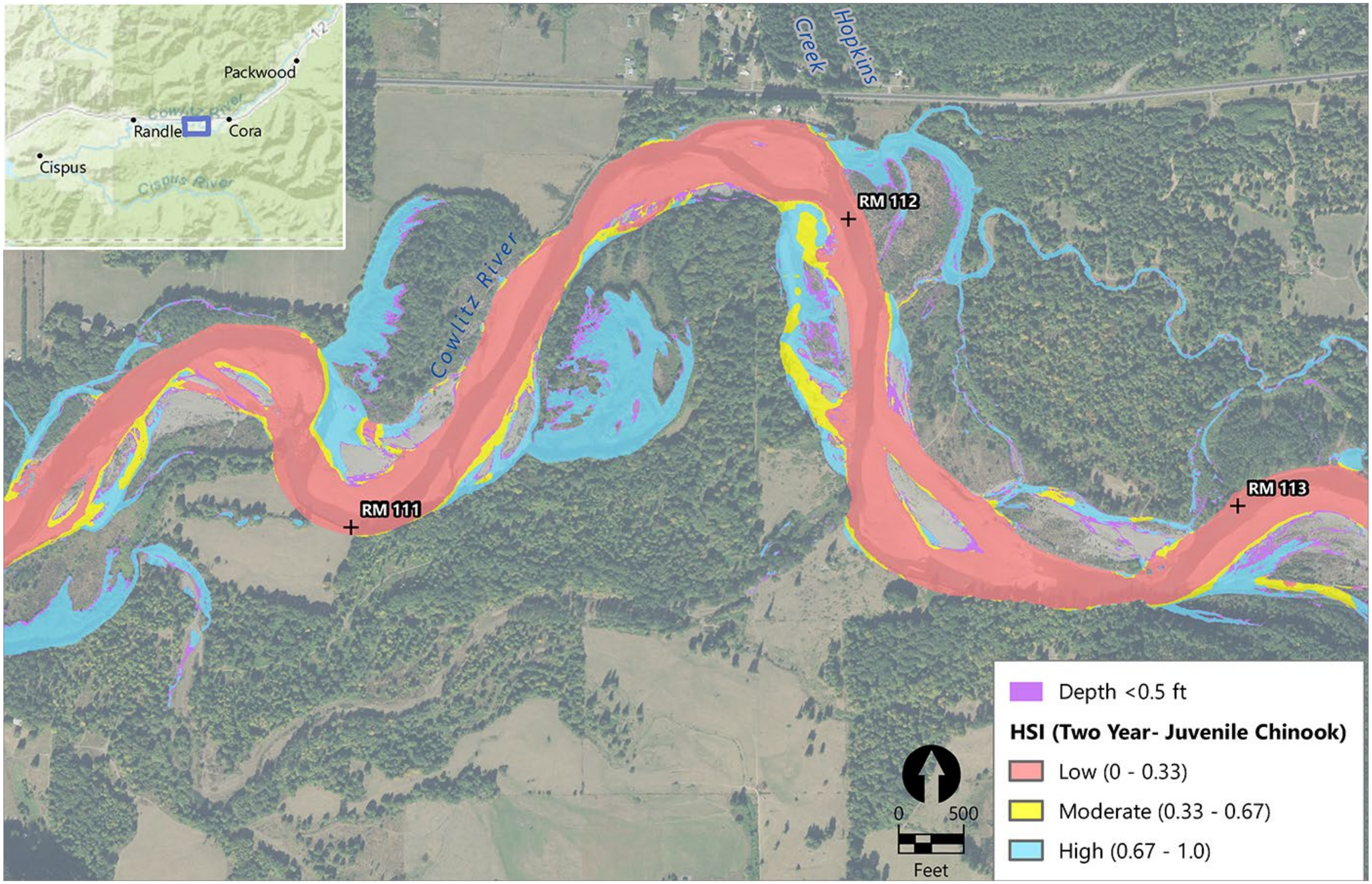

**Figure 6-3**
**Predicted HSI Results in the Upper River Basin – 2-Year Flood Event – Juvenile Steelhead**

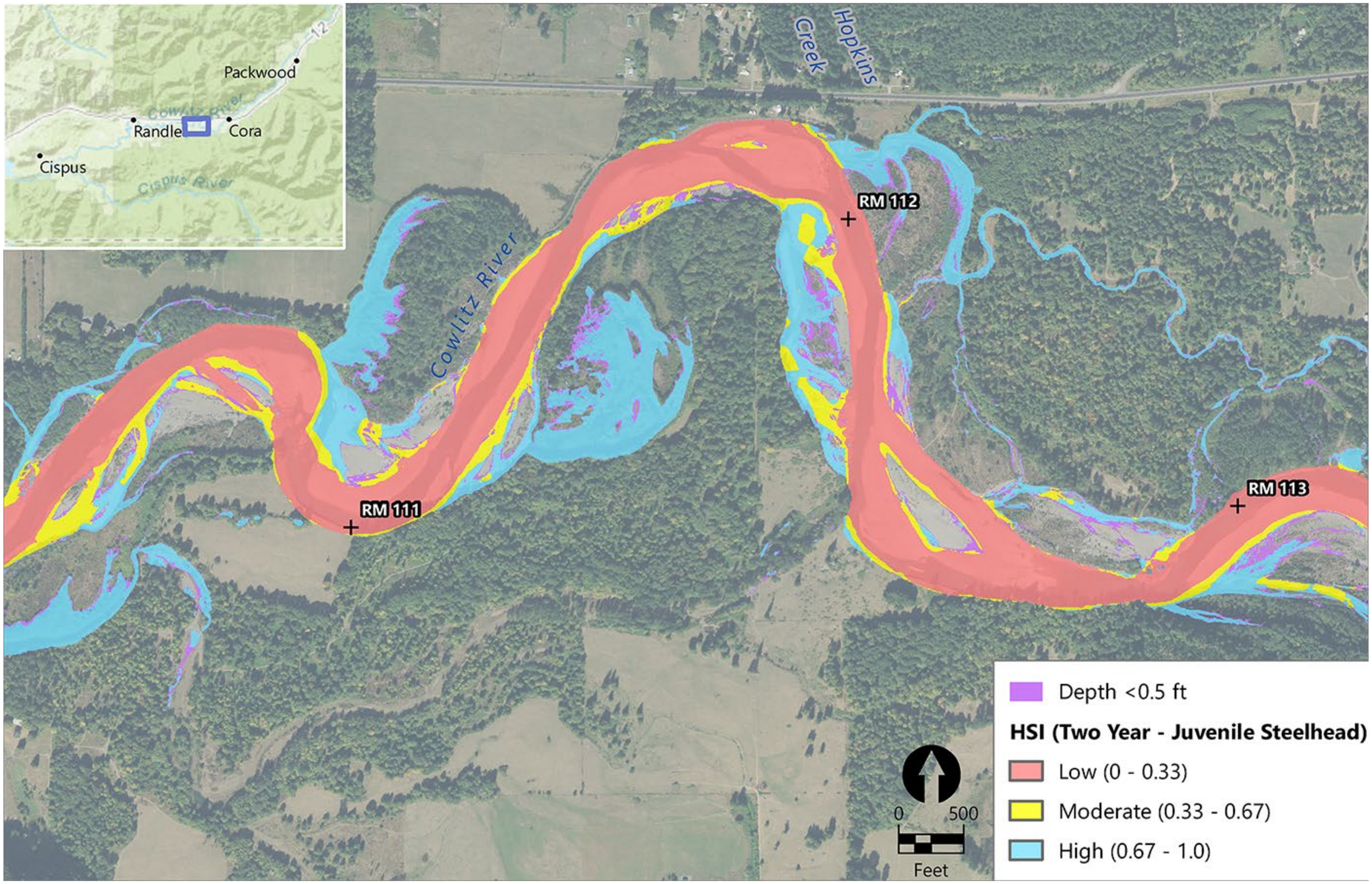

## 6.3 Habitat Suitability Index Summary

Tables 6-4a and 6-4b summarize the HSI results by area in each focus area of the model (lower area near Randle, middle area, and upper area near Packwood) for juvenile Chinook salmon and juvenile steelhead, respectively.

These results show that the area of high HSI habitat increases significantly during the 2-year flood, due to the inundation of side channels (upper area) and former avulsion channels (middle and lower areas). During summer low flow conditions Chinook salmon shower higher suitability in the middle and upper areas, while steelhead have more area of high HSI in the lower area near Randle. For the winter average high flow and 1-year flood conditions, the area of high HSI values decreases due to the channelization of flows without enough flow to connected to former avulsion and backwater areas. Steelhead have more area of moderate suitability habitat in the lower and middle areas, compared to Chinook salmon, which experience more area of low HSI in these areas and only slightly more low suitability habitat in the upper area compared to Chinook salmon.

**Table 6-4a**
**Summary of Habitat Suitability Area (Acres) – Juvenile Chinook Salmon**

| Model Area | Area Length (River Miles) | Summer Average Low Flow | | | Winter Average High Flow | | | Annual (1-Year) Flood | | | 2-Year Flood | | |
|---|---|---|---|---|---|---|---|---|---|---|---|---|---|
| | | Low | Moderate | High | Low | Moderate | High | Low | Moderate | High | Low | Moderate | High |
| Lower Area (near Randle) | 5 | 43 | 65 | 108 | 146 | 73 | 38 | 223 | 37 | 61 | 346 | 26 | 303 |
| Middle Valley Area | 12 | 109 | 83 | 75 | 245 | 57 | 37 | 353 | 35 | 58 | 488 | 40 | 219 |
| Upper Area (near Packwood) | 7 | 108 | 26 | 20 | 171 | 12 | 26 | 223 | 12 | 51 | 348 | 48 | 109 |

Note:

1. The 10-year flood simulation was not evaluated for HSI due to the relative infrequency of this event.

**Table 6-4b**
**Summary of Habitat Suitability Area (Acres) – Juvenile Steelhead**

| Model Area | Area Length (River Miles) | Summer Average Low Flow | | | Winter Average High Flow | | | Annual (1-Year) Flood | | | 2-Year Flood | | |
|---|---|---|---|---|---|---|---|---|---|---|---|---|---|
| | | Low | Moderate | High | Low | Moderate | High | Low | Moderate | High | Low | Moderate | High |
| Lower Area (near Randle) | 5 | 23 | 67 | 126 | 66 | 143 | 48 | 167 | 87 | 67 | 317 | 51 | 307 |
| Middle Valley Area | 12 | 63 | 110 | 93 | 165 | 129 | 45 | 304 | 78 | 64 | 453 | 67 | 228 |
| Upper Area (near Packwood) | 7 | 80 | 51 | 24 | 154 | 27 | 28 | 211 | 22 | 53 | 314 | 71 | 120 |

Note:

1. The 10-year flood simulation was not evaluated for HSI due to the relative infrequency of this event.
2. Differences in the total areas for each flow conditions are due to rounding. Total wetted area evaluated for HSI for each species was the same.

# 7 Channel Complexity Evaluation

Channel and floodplain complexity have increasingly been associated with favorable habitat areas for juvenile salmonid rearing and overwintering, as well as benefits for many other aquatic species in the riverine system. Because of this multi-species and multi–life stage benefit, it is important to examine a reach's complexity at several different flow levels—typically at lower, sustained flows (see Table 7-1). For this analysis, complexity or channel complexity refers to the geomorphic condition of multi-threaded or anastomosing channels, side channels, and split flow. Complexity is often characterized by small, dynamic side channels and sinuous meandering main channels that interact freely with the surrounding floodplain. While greater complexity typically results in a larger total water surface area, it is distinct from floodplain connectivity in that it examines individual flow paths separated by floodplain.

**Table 7-1**
**Flow Used for Examining Complexity**

| Flow Description | Data Source | Flow Rate at Randle |
|---|---|---|
| Summer average | 2D Hydraulic Model | 1,360 cfs |
| Winter average | 2D Hydraulic Model | 3,670 cfs |
| 1-year flood event | 2D Hydraulic Model | 7,100 cfs |

When complexity is maintained during summer low flows and winter flows, it indicates that side channels, backwaters, and other off channel areas that are important for a variety of ecological process are sustained for longer periods of time and will therefore provide these ecological benefits including juvenile salmonid rearing for a large portion of the hydrograph. While the 1-year flow is episodic in nature, maintaining complexity at this flow level is important for both the geomorphic and ecological processes of the system. Channel systems that maintain and reoccupy alternative channels during high-flow events create geomorphically resilient systems that mobilize sediment stored in the floodplain and recruit wood material from riparian areas, both key aspects of the natural processes of a riverine system. Furthermore, the lower velocity channel alternatives, and backwaters indicated by complexity, provide essential hydraulic refugia for fish during these high flow events. These three flows should represent the normal range of river conditions where habitat benefits from complexity are most relevant for juvenile salmonids.

## 7.1 Methods Summary

For this complexity evaluation, six complexity assessment areas were delineated within the study area for analysis. Theses area were delineated based on similarity in geomorphic properties as well as the individual parts of complexity described below: sinuosity, island density, and island size. Keeping area of similar complexity together is important for this analysis in order to prevent an area with both good and bad complexity washing out and showing only average complexity. Throughout this section these areas will be referred to as "reaches," which is used as a general term for discrete units of a river length, rather than referring to the three reaches described above.

The concept for the Standardized Complexity Evaluation (SCE) discussed in this section was largely influenced by the River Complexity Index (RCI) shown in Equation 7-1. RCI is a method of measuring complexity at bankfull flow proposed by Brown and others (Brown 2002; Beechie et al. 2017; USFS 2012). The method takes the product of reach sinuosity and node density, a measure of channel connections in a reach. A more complete explanation of the RCI method can be found in "River Complexity Index (RCI): A Standard Method" (Buelow et al. 2017).

**Equation 7-1**

$$RCI = S * (1 + D) = \left(\frac{Main\ Channel\ Length}{Valley\ Centerline\ Length}\right) * \left(1 + \frac{Number\ of\ Stream\ Nodes}{Valley\ Centerline\ Length}\right)$$

where:

| | | |
|---|---|---|
| RCI | = | River Complexity Index for a reach |
| S | = | sinuosity of the reach |
| D | = | node density of the reach |

Note:
RCI equation from "River Complexity Index (RCI): A Standard Method" (Buelow et al. 2017). Originally developed by Brown (2002).

The SCE developed in this analysis draws from the basic parameters of RCI by using the sinuosity of the reach and the number of islands in the reach. The nodes described in the RCI method are difficult to capture and define using LiDAR-produced digital elevation models and GIS data-processing techniques. However, because every pair of nodes represents an island, counting the number of islands per reach can be used as a scalable representation for node density, as shown in Figure 7-1. Islands can be easily recognizable as distinct polygons in GIS applications, and statistics on where and how big these islands are can be quickly generated. Water surface polygons for the low flow, winter flow, and 1-year flow were generated using a 2D HEC-RAS model and the direct outputs from the LiDAR water surface data. For a complete discussion on the modeling, see Section 4.1.

For this assessment, only islands with a length greater than the average channel width for each of the respective reaches were counted toward this metric to remove any short side channels or areas that form small mid-channel bars. It should be noted that, because islands were used instead of nodes, the complexity values produced by this analysis are not directly comparable to the RCI method. Minimum island lengths for each evaluated flow conditions were calculated, and a single minimum island length of 150 feet was chosen to be representative of the study area. While average channel width varies by reach and flow event, choosing a single value allows for complexity values to be comparable across these different reaches and flow events. The length of 150 feet represents the smallest of average channel widths found, but still represents an island that would pose significant contributions to the overall complexity.

However, in the SCE, in addition to sinuosity and island density, a third parameter was used to characterize complexity: island perimeter length. Through experience using this analysis on other river systems (e.g., the Tucannon River and Touchet River), it has been observed that reaches with long side channels tend to score more poorly in the complexity analysis than expected from field observations when using only sinuosity and island density. While a single long side channel may not represent as much complexity as many smaller side channels and split flows, it does represent significantly more complexity than a confined single thread channel. Therefore, the island perimeter length parameter was added into the calculation of complexity in this methodology to account for these situations, as well as to provide a more complete and accurate view of complexity within the assessment area. Figure 7-2 shows a general trend of increasing complexity with both the number of islands and the total perimeter length of the islands.

**Figure 7-1**
**Cowlitz River Complexity Assessment Areas**

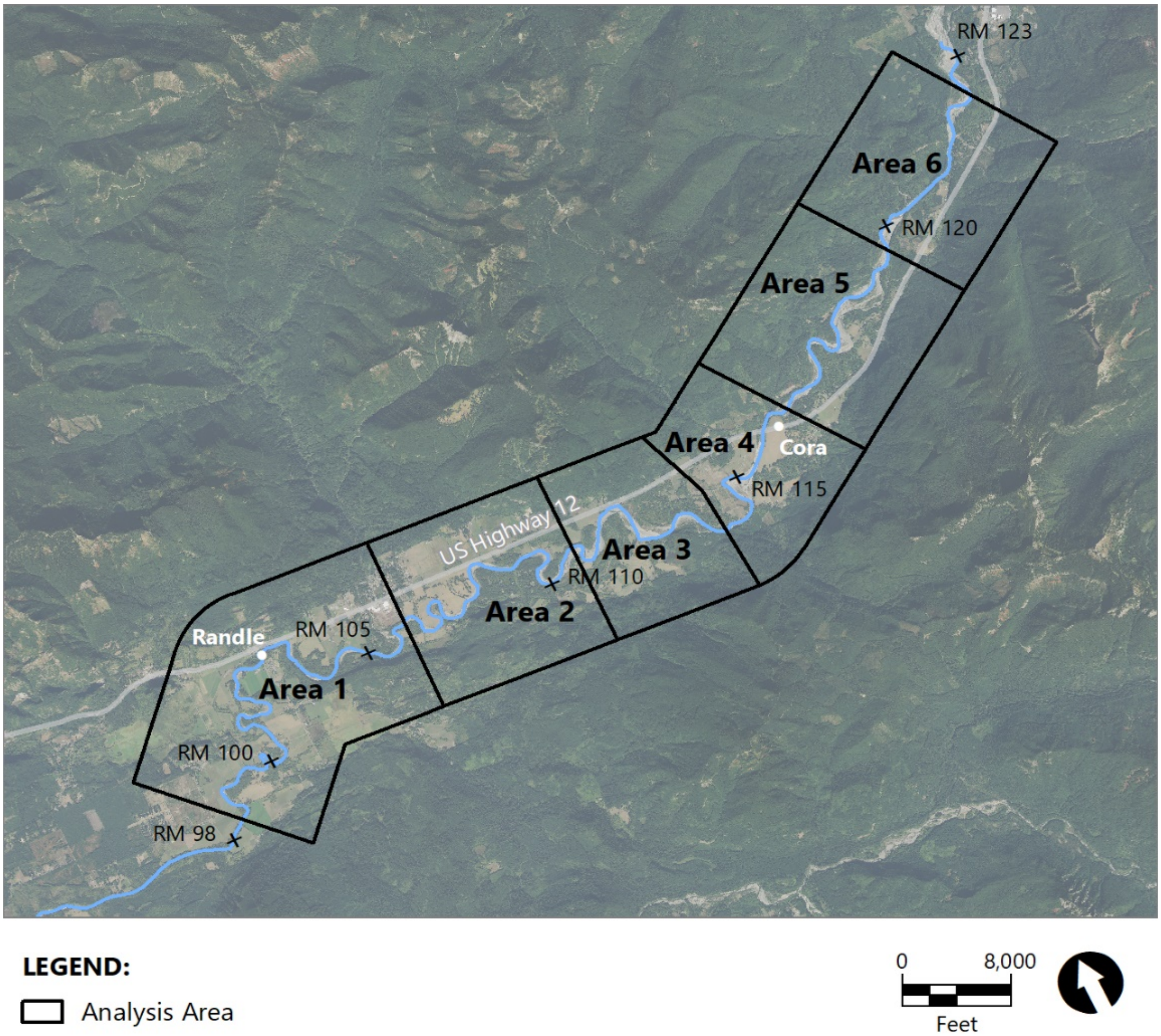

**Figure 7-2**
**Complexity Comparison**

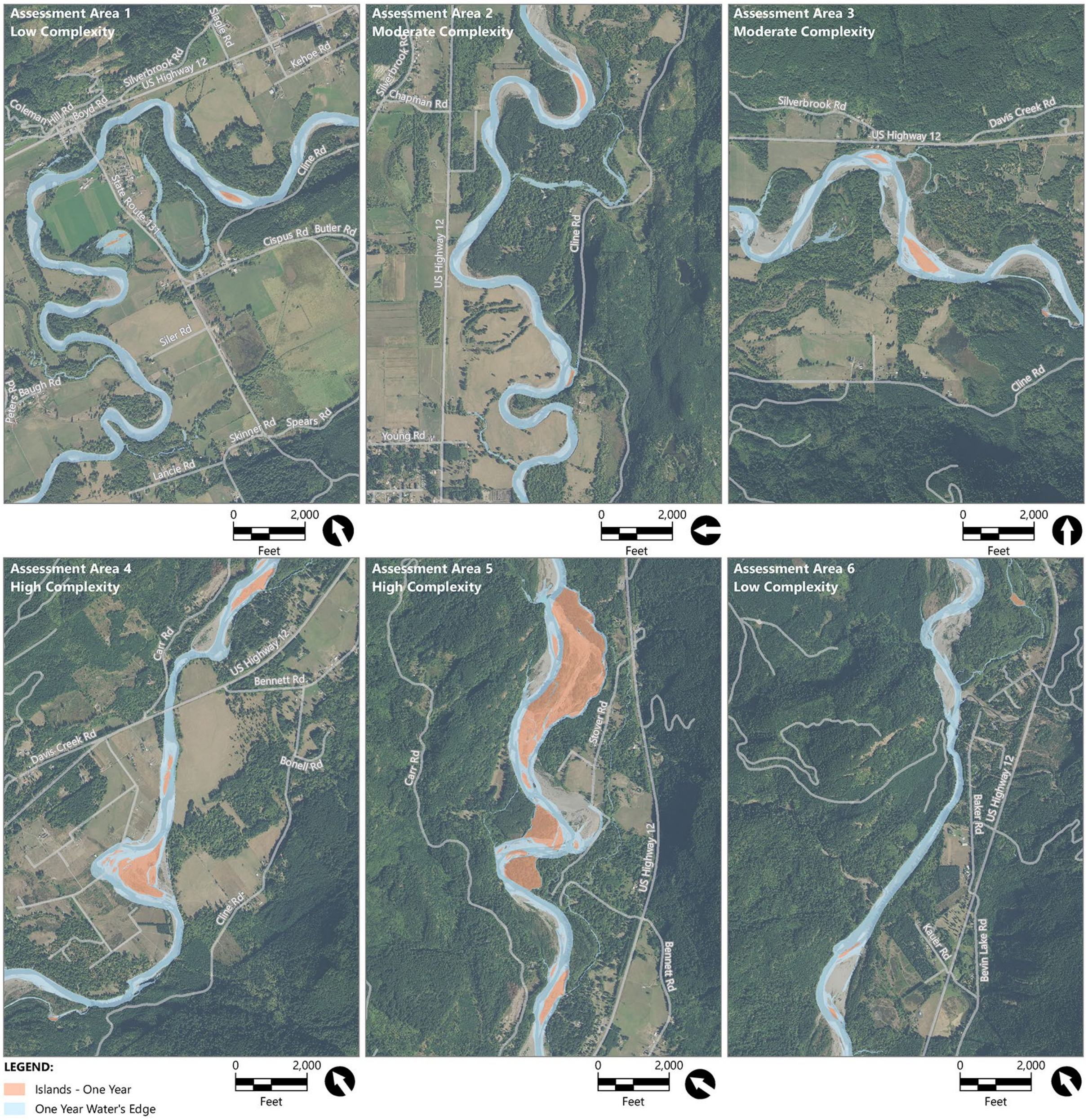

The complexity evaluation used in this analysis sums these three parameters, as shown in Equation 7-2. In order to account for differing reach lengths, each parameter was divided by the length of the valley (already included in the calculation of sinuosity) and standardized such that the maximum value across all three flows examined was 1. The benefit of standardizing all three parameters allows for each parameter to be examined initially on an equal footing, without weighting any parameter without purpose. After the standardization, with the SCE it is then possible to choose weighting factors based on the perceived importance toward complexity.

**Equation 7-2**

$$W_s(\mathrm{S}) + W_i(\mathrm{I}) + W_p(\mathrm{P}) = \text{Standardized Complexity Evaluation (SCE)}$$

where:

| | | |
|---|---|---|
| $W_x$ | = | weighting factor for the given parameter |
| S | = | standardized sinuosity per project area |
| I | = | island count per valley length per project area, standardized across all three flows |
| P | = | island perimeter per valley length per project area, standardized across all three flows |

The utility of this tool is that these factors can be weighted differently, and the amount of influence a specific factor has on the complexity evaluation can be changed based on a specific need. As shown in Equation 7-2, each of these parameters was weighted (0.4 for island count, 0.2 for island perimeter, and 0.4 for sinuosity) based on the following lines of reasoning on the importance of each parameter to the complexity of the study area. In this section of the Cowlitz River basin, sinuosity plays a major role in the complexity of the reach, where the meander and length of the river defines its connection and interaction with the floodplain shoreline. Mid-channel islands and vegetated bars similarly play an important role in the complexity of these reaches, especially when split flows have near-equal flow ratios. Long side channels are less common in this river system and are typically much lower in flow capacity relative to the mainstem of the Cowlitz, decreasing their importance to habitat.

It should be noted that, because of the way the complexity index is calculated, the resulting values are comparable only to other reaches in this analysis. Should this method be applied to other river systems, the resulting values would only be relative to that system. This method is not meant to compare complexity between river systems but rather to examine the complexity of a reach compared to other reaches within the system. Furthermore, the selection of these specific parameters and weighting factors is tailored to the Cowlitz River system, its geomorphic processes, and unique history, and may need modification before applying to other systems.

## 7.2 Complexity Trends and Patterns

This section briefly describes some of the trends and findings from the complexity analysis. River complexity shows several trends across the assessment area. Most of the assessment reaches in this assessment area do not vary much between the three flows. Sinuosity shows a consistent trend upward looking from upstream to downstream as shown in Figure 7-3. This is to be expected as the river comes out of the higher gradient reaches 5 and 6, and transitions into the lower gradient and more open big valley in Reaches 1 to 4. In Figure 7-4, Reaches 1 to 3 maintain a relatively constant moderate complexity value moving upstream, being largely controlled by their high sinuosities. It should be noted that just downstream of Reach 1 the channel becomes much more single thread and less sinuous, likely due to the fact that this reach is under backwater control from Lake Scanewa. In Figures 7-5 and 7-6, island count and perimeter length show a general trend of increasing from the downstream Reach 1 until about Reach 4 or 5 where these parameters peak. Reach 6, river miles 120 to 122, shows very low island count and perimeter length values, again likely due to the fact that this reach is still in the steeper gradient zone before the depositional area of the valley.

**Figure 7-3**
**Sinuosity Across Reaches 1 to 6**

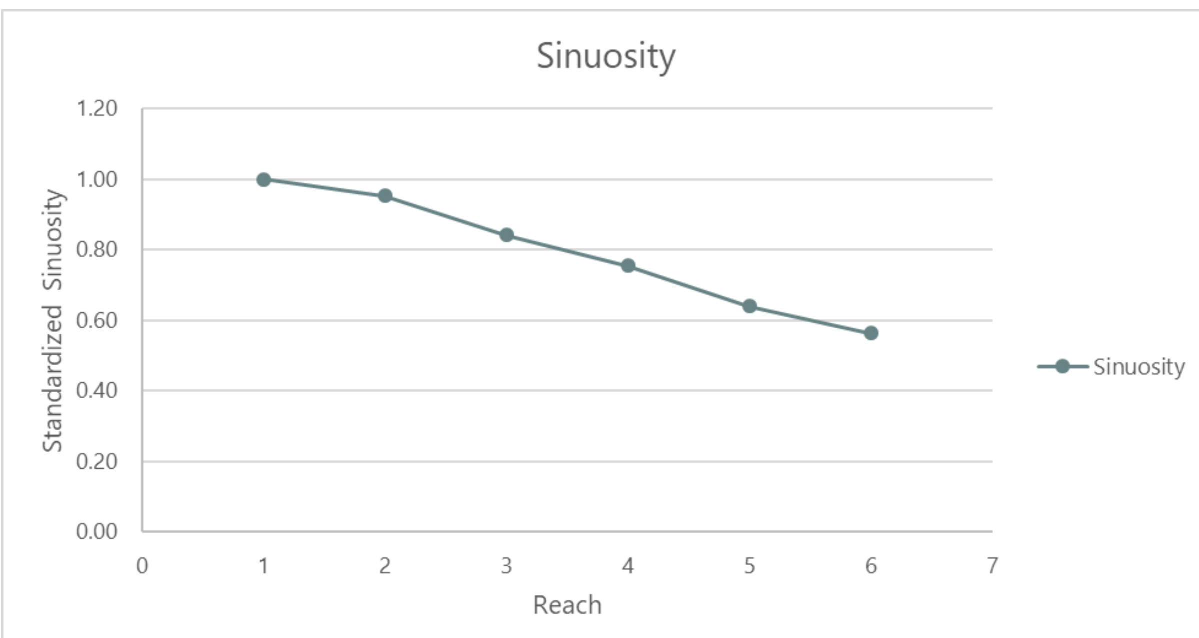

For total complexity between the three flows, only Reach 4 shows much increase in complexity, with the other reaches remaining relatively constant across all three flows, as shown in Figure 7-4. Reach 5 is the only location where the three flows do not follow a similar trend. During winter and summer flows the complexity in Reach 5 is similar to the levels seen in Reaches 1 to 3. However, during the 1-year flow complexity is at its highest in Reach 5, which could indicate the presence of high flow side channels only activated at a 1-year flow. In the downstream Reaches of 1 to 3 the moderate complexity values is again likely due to the fact that the complexity in these reaches is largely controlled by their higher sinuosity, with only a slight increase in the number of islands across the three flows. This could indicate that many of the side channels are perennial at lower flows as well as stable and not flooded out at higher flows. It may be possible that these well-defined flow paths exist in this area, without leaving more room for the river to activate additional flow paths.

**Figure 7-4**
**SCE Across Reaches 1 to 6**


In Figure 7-4, Reaches 4 and 5 show the increase in complexity as flows increase that might be conventionally expected. Because main channel sinuosity remains relatively constant across all flows, these changes are likely due to higher-flow side channels in the floodplain becoming activated especially in Reach 5 at the 1-year event. Island count, shown in Figure 7-5, and perimeter length, shown in Figure 7-6, show a sharp increase in Reach 4 for all flow events, which is maintained in Reach 5 only during the 1-year flow event. This indicates that Reach 4 has high sustained complexity across flow events with side channels and sinuosity being maintained even at lower flows. However, in Reach 5, the high amount of side channels connected only at the 1-year event indicates that alternate flow paths exist in this reach, and that it has the highest potential for increasing complexity at the lower flows as well, raising the overall complexity of the reach.

**Figure 7-5**
**Island Count Across Reaches 1 to 6**

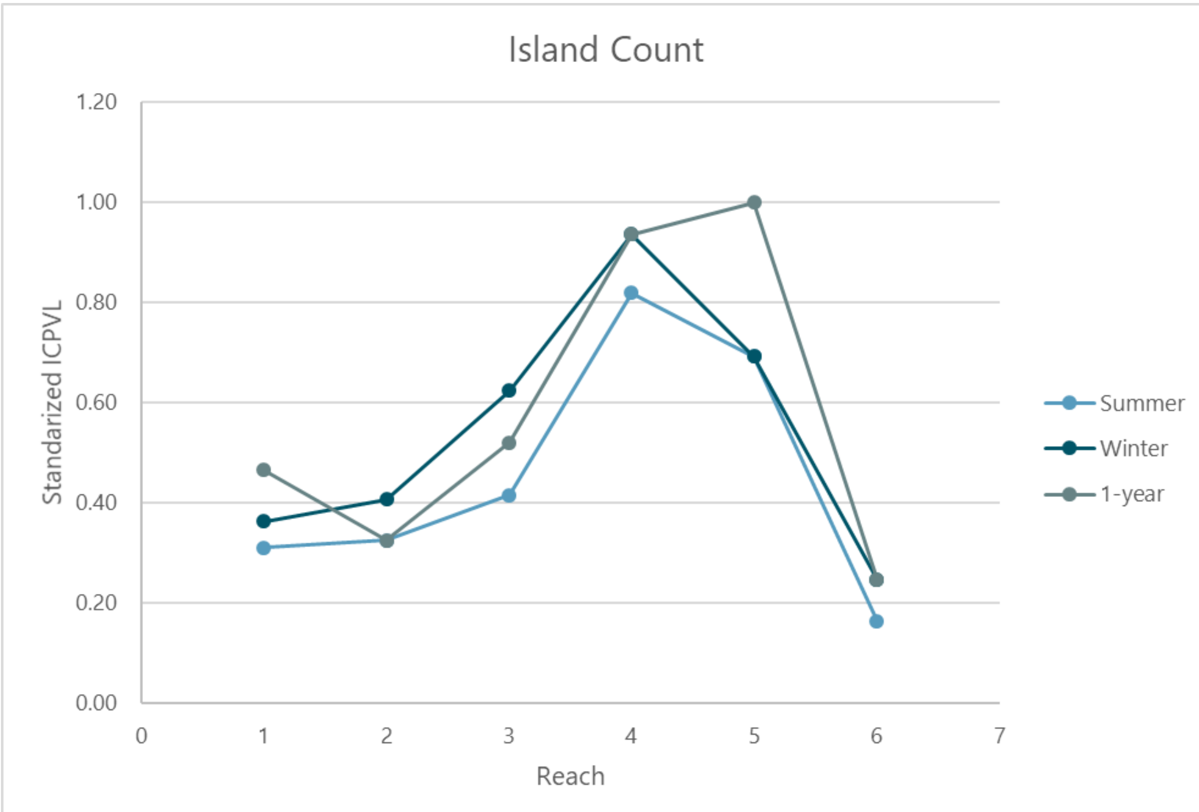

**Figure 7-6**
**Perimeter Length Across Reaches 1 to 6**

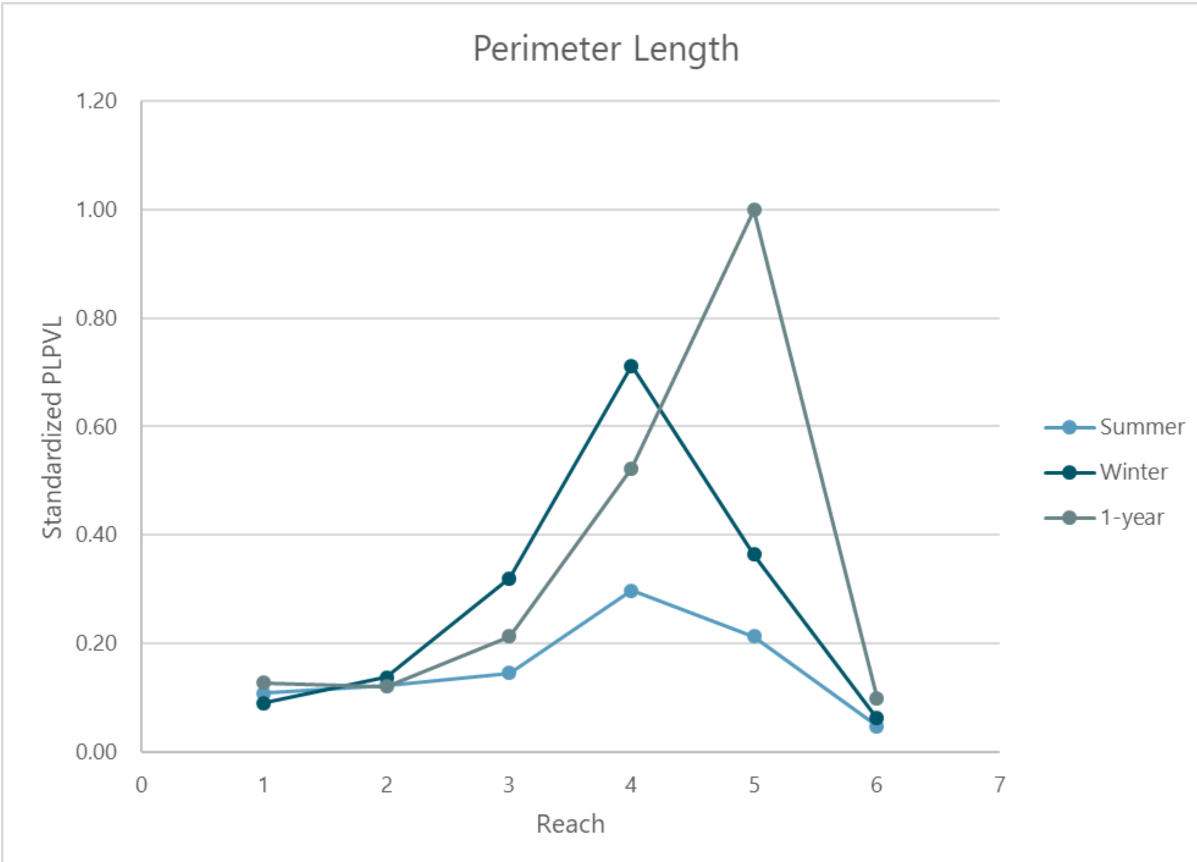


Interestingly, the island perimeter length at the winter flow is higher than both the summer and 1-year flow for several reaches. This result suggests that many of the side channels and low-flow paths in the floodplain are not being inundated at the lowest flow events, but then are also partially washed out and inundated at the highest flow event as discussed previously. Lowering these side channels and stabilizing them at high flows could be a target for restoration efforts seeking to increase complexity and overall habitat area at lower flows. A failure to maintain complexity risks losing aquatic habitat area and habitat quality throughout the year. Maintaining complexity could potentially be accomplished by providing structure on the existing islands to promote long-term sediment storage and mature forests.

# 8 Assessment of Preliminary Habitat Restoration Alternative

Anchor QEA applied the fine-scale 2D hydrodynamic model to evaluate a preliminary habitat restoration alternative developed with Tacoma Power for improvements to habitat suitability. The results of that habitat alternative assessment are provided in Appendix B.

# 9 References


Beechie, T.J., O. Stefankiv, B.L. Timpane-Padgham, J.E. Hall, G.R. Pess, M.L. Rowse, M.C. Liermann, K.L. Fresh, and M.D. Ford, 2017. *Monitoring Salmon Habitat Status and Trends in Puget Sound: Development of Sample Designs, Monitoring Metrics, and Sampling Protocols for Large River, Floodplain Delta, and Nearshore Environments*. U.S. Department of Commerce, NOAA Technical Memorandum NMFS-NWFSC-137. https://doi.org/10.7289/V5/TM-NWFSC-137.

Brown, A.G., 2002. "Learning from the past: palaeohydrology and palaeoecology." *Freshwater Biology* 47:817–829.

Buelow, K., K. Fischer, J. O'Neal, Z. Seilo, and R. Ventres-Pake, 2017 [unpublished]. "River Complexity Index (RCI): A Standard Method."

Chow, V.T., 1959. *Open-Channel Hydraulics*. New York: McGraw-Hill.

FEMA (Federal Emergency Management Agency), 2006. *Flood Insurance Study*. Lewis County, Washington. Volumes 1 to 3. July 17, 2006.

QSI (Quantum Spatial, Inc.), 2018. *Cowlitz River, Washington Topobathymetric LiDAR Technical Data Report*. July 20, 2018.

USACE (U.S. Army Corps of Engineers), 2016. *HEC-RAS River Analysis System 2D Modeling User's Manual, Version 5.0*. February 2016.

U.S. Forest Service (USFS), 2012. *Stream Inventory Handbook: Level I and Level II*. USFS Pacific Northwest Region (Region 6). Version 2.12, 127p.

USGS (U.S. Geological Survey), 2016a. National Geospatial Data Asset (NGDA) Land Use Land Cover. Available at: https://catalog.data.gov/dataset/usgs-land-cover-nlcd-overlay-map-service-from-the-national-map-national-geospatial-data-asset-50f25.

USGS, 2016b. Scientific Investigations Report 2008 -5093. Table 7. Available at: https://pubs.usgs.gov/sir/2008/5093/table7.html

Washington Department of Fish and Wildlife (WDFW), 2016. *Instream Flow Study Guidelines: Technical and Habitat Suitability Issues Including Fish Preference Curves*. Department of Fish and Wildlife and Washington State Department of Ecology. March 2016.

# Appendix A
# Coarse-Scale Model Development and Results

1605 Cornwall Avenue
Bellingham, Washington 98225
360.733.4311

ANCHOR QEA

# Memorandum

December 17, 2018

To: Florian Leischner, Tacoma Power

From: Kyle List, PE, and Tracy Drury, PE, Anchor QEA, LLC

**Re: Cowlitz River Restoration and Recovery – Task 1: Coarse Level Hydraulic Model Development**

## Hydraulic Model Development

As part of the Cowlitz Restoration and Recovery Habitat Assessment, Anchor QEA was tasked with the development of a coarse-scale hydraulic model for the Upper Cowlitz River and floodplain basin. The hydraulic model was developed using the site-wide topo-bathymetric aerial light detection and ranging (LiDAR) survey (QSI 2018), which included the Cowlitz River bathymetry and floodplain basin topography extending from the Cowlitz Falls dam and Lake Scanewa upstream to approximately 2 miles south of Packwood, Washington. The one-dimensional (1D) model spans this area and will be used to further evaluate restoration opportunities using a high-resolution hydraulic model in targeted reaches as part of Task 2. This memorandum describes the development of the Upper Cowlitz River basin 1D hydraulic model as well as the limited validation of the coarse scale model hydraulic predictions.

### LiDAR and Supplemental Elevation Data

The topo-bathymetric ("blue-green") LiDAR data were collected with an aerial based scanner on April 24 and 25, 2018, by Quantum Spatial (QSI 2018) and provided to Anchor QEA as digital surface data for use as the channel and floodplain geometry of the hydraulic model. Data were collected using the North American Vertical Datum of 1988 (NAVD 88). Topographic LiDAR coverage of the Upper Cowlitz River floodplain provides highly detailed and complete coverage of the basin. The LiDAR was able to penetrate between 5 and 10 feet beneath the surface of the water in the channel and provide good data coverage for the upper portion of the LiDAR. Near Randle, Washington, water levels were deeper than the upper reaches and some data gaps were observed in the deepest pools of the channel. Bathymetry data were not provided for the downstream sections of the Upper Cowlitz, including the areas influenced by Lake Scanewa to the Cowlitz Falls dam, due to the water depths which were greater than the LiDAR's penetrating capabilities.

To more accurately represent bed elevations of deeper pools, an interpolation method was used to estimate elevations in the areas of missing data. Longitudinal profiles were interpolated between the upstream to downstream end of the missing data. The profile lines were then used to patch the areas of missing bathymetry by interpolating from either side of the river bank where data were available. In the downstream backwater areas, the thalweg profile from the 2006 Federal Emergency

Management Agency (FEMA) Flood Insurance Study (FIS) (FEMA 2006) for Lewis County was used to generate the channel bottom profile and the channel geometry was approximated and joined with the topographic data. Anchor QEA expects that additional surveys will be required to ground-truth the approximations of the river channel bathymetry that was used to supplement the LiDAR topo-bathymetric data. The extents of the model and the final model elevation "surface" are shown in Figure 1.

**Figure 1**
**Model Combined Topography and Bathymetry Surface**

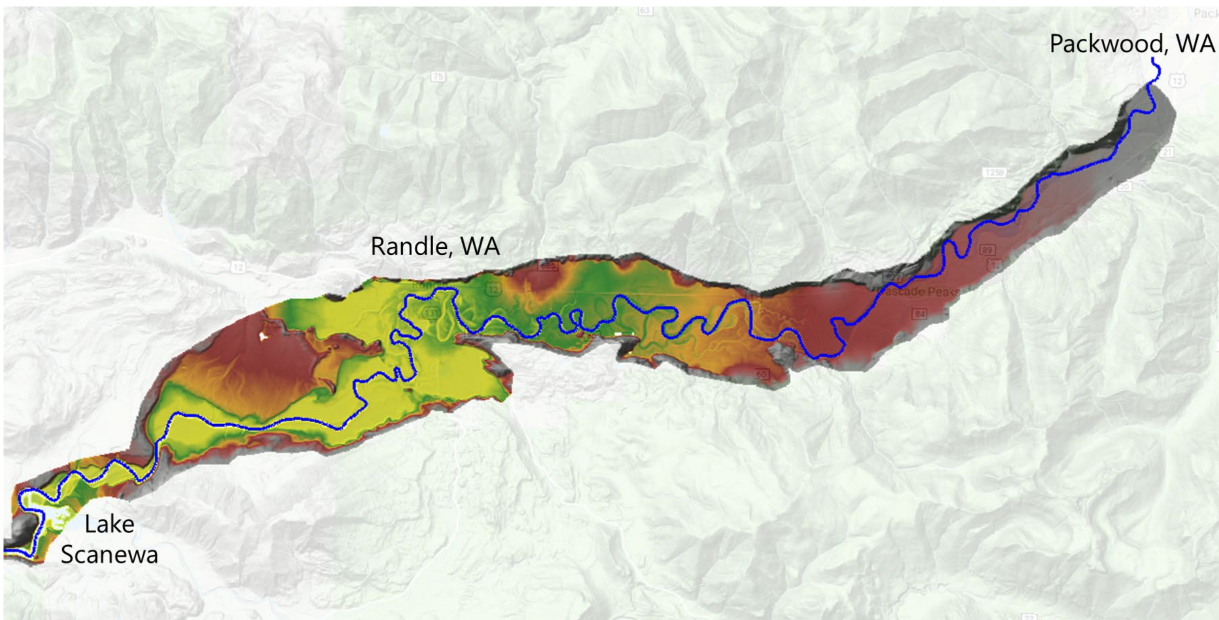


## Model Geometry Development

The U.S. Army Corps of Engineers (USACE) HEC-RAS version 5.0.5 was used as the modeling framework. While capable of computing 2D hydrodynamics, the model was developed solely in 1D mode using a total of 236 cross sections spaced approximately every 400 to 800 feet along the river to represent the 2D data surface geometry. Figure 2 shows an overview of the model cross section locations.

**Figure 2**
**Hydraulic Model Transect Geometry (1D)**

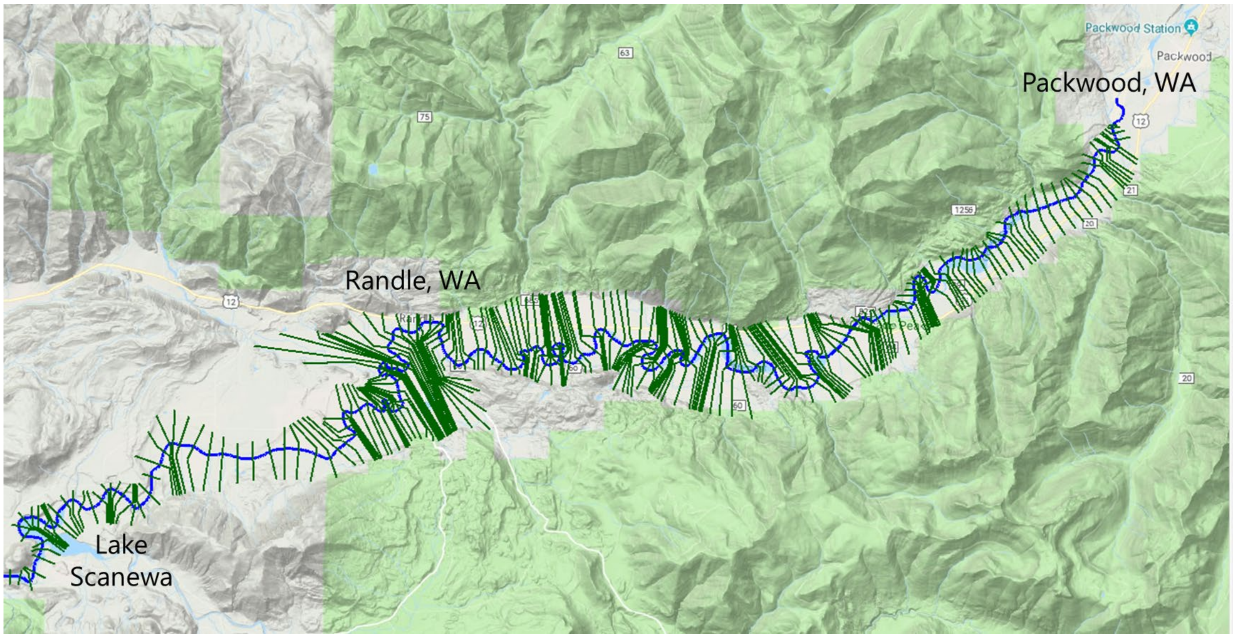


Note: Green lines represent the model cross sections.

Bridge data measurements for the Route 131 and Route 12 bridge crossings were not available as part of this study, so bridges were included in the model using additional transects to capture the hydraulic effects of the abutments. The Manning's n empirical roughness coefficients for the channel and floodplain were selected based on the recommended values from the Lewis County FIS.

## Preliminary Hydraulic Results

Steady state 1D model simulations were performed for return interval flow rates including low flow (during the period of the LiDAR survey in April of 2018) and flood events ranging from the 2-year to the 100-year flood event. The flow rate was used as the upstream boundary condition input into the model. The downstream boundary of the model is controlled by the pool level for Lake Scanewa, which is controlled by the flow through the Cowlitz Falls dams. The pool elevation is variable based on the flow rate in the river. The pool elevations were provided by Tacoma Power and were used as the downstream boundary condition for the model, and the hydraulic flow through the dam was not included as part of this study. The results of the predicted hydraulics will be evaluated in detail as part of Task 2.

### Model Validation

Since calibration and validation gage data were not available for the scope of this modeling effort, a simple validation of the results for low flow conditions was performed to ensure the model is accurately predicting flow within the channel banks prior to evaluating overtopping of the channel during higher flow model simulations. The flow rates during the LiDAR survey measurements were obtained from the Packwood and Randle U.S. Geological Survey flow gages (Stations #14226500 and # 14231000, respectively), and the model-predicted water depths were compared to the boundary of the water in the channel determined as part of the LiDAR survey post-processing (see Figure 3). The predicted extents of flow in the channel show good agreement with the boundary of the wetted areas from the LiDAR survey.

**Figure 3**
**Predicted Submerged Areas versus LiDAR Survey Water Boundary**

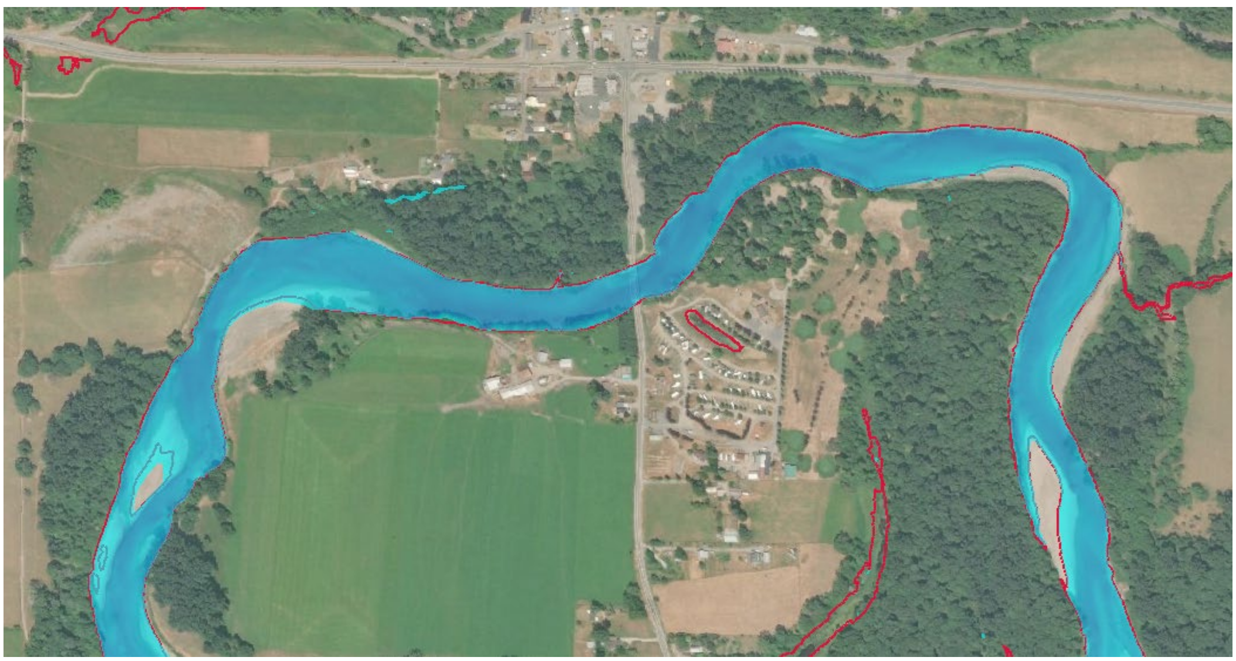

Note: Results are shown near Randle, Washington. Red lines show the extent of water determined by the LiDAR survey. Blue areas show areas predicted to be inundated by the model for the date of the LiDAR simulation flights.

## Flood Evaluation

In addition to low flows, the 100-year water surface elevation profile predicted by the model was compared to the water surface elevation profile of the regulatory 100-year flood reported in the FEMA FIS report (See Figure 4). The model shows generally good agreement with the regulatory flood stage, with the areas of best agreement being near the most sinuous locations of the river near Randle, Washington. This area has close spacing of the FEMA profile transects and good coverage from the topo-bathymetric LiDAR survey (minimal gaps in the deep areas of the channel). The downstream elevations use the patched data for the channel bathymetry, and in this location the predicted 100-year flood stage is slightly greater than the regulatory flood stage. Approximately 4 miles upstream of Randle, the predicted stage becomes lower than the regulatory flood stage. This is likely due to the extremely sparse spacing of the FEMA model in this area.

**Figure 4**
**Water Level 100-year Comparison with FEMA FIS Flood Profile**

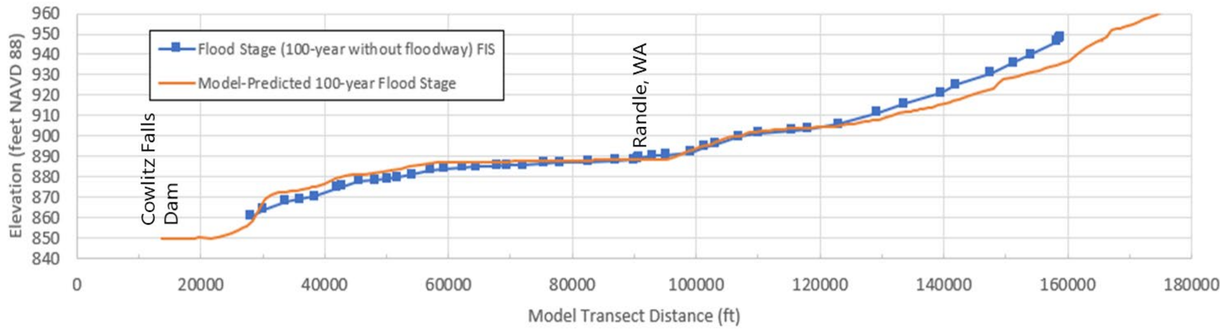


# References

FEMA (Federal Emergency Management Agency), 2006. Flood Insurance Study. Lewis County, Washington. Volumes 1 to 3. Federal Emergency Management Agency. July 17, 2006.

QSI, 2018. *Cowlitz River, Washington Topobathymetric LiDAR Technical Data Report*. July 20, 2018.

# Appendix B
# Randle Side Channel Modeling Evaluation

1605 Cornwall Avenue
Bellingham, Washington 98225
360.733.4311

ANCHOR QEA

# Memorandum

March 31, 2020

To: Florian Leischner and Melora Shelton, Tacoma Power

From: Tracy Drury, Kyle List, and Tom Hutchison, Anchor QEA, LLC

**Re: Cowlitz River Restoration and Recovery, Task 4: Randle Side Channel Modeling Evaluation**

## Introduction and Methods

### Purpose

This memorandum presents results from the most recent modeling effort comparing existing conditions and proposed alternatives to reconnect a side channel on the upper Cowlitz River just downstream of Randle, Washington. It illustrates how the hydraulic model can technically evaluate restoration alternatives and communicate potential outcomes to interested parties including restoration practitioners, community members, and regulators. This exercise does not identify a preferred restoration action and this restoration concept has not been evaluated by Lower Columbia Fish Recovery Board or Tacoma Power recovery initiatives or habitat strategies. It has not been vetted with potentially affected landowners, which include both private and public entities. This side channel reconnection concept was identified by the Upper Cowlitz and Cispus Technical Work Group during the recent habitat strategy development (Lower Columbia Fish Recovery Board 2019), but was not developed further due to landowner concerns. Tacoma Power returned to this concept for this memorandum because it offered both potential habitat benefit and opportunity to explore how modeling could help evaluate and communicate results and address concerns including potential farm field flooding, increased erosion risk, and conflicts with existing land use.

The objectives of this conceptual design were twofold: to promote connectivity of an existing side channel and to mitigate flooding in adjacent farm fields. Increasing the inundation frequency of the side channel provides increased salmonid habitat benefit, especially for juveniles to use the side channel as a low-velocity refuge during high flow events. Backwater and side channel habitats are key rearing habitats for juvenile salmonids because they provide low velocities and cover from predators. The flood reduction component of the design was achieved with channel excavation to create a flow path from the upstream to downstream portions of the existing side channel, as noted in the more downstream cut location in Figure 1. In the existing condition, flow backs up at the upstream end of the side channel and spills directly into farm fields. Creating a flow path helps reduce the magnitude and duration of flooding in the fields. To optimize the design to meet both criteria, multiple iterations were made to alter the width, length, and location of the excavated channel cuts. Three design alternatives were modeled and compared with the existing conditions to assess their effectiveness in fulfilling the two design criteria.

The results from the modeling effort were used to compare differences in flow velocity, flooding extent, and the return interval that results in connected flow among the existing conditions and proposed alternatives. Alternatives were designed to reconnect the 1.8-mile-long side channel in the right floodplain. The channel cuts of the three alternatives varied from 0.3 to 0.4 mile in length. An overview of the site showing the existing side channel flow path and proposed cut locations is shown in Figure 1. As seen from the aerial imagery, agriculture is the primary land use in the floodplain in the Randle reach, and the river frequently floods low-lying agricultural fields.

**Figure 1**
**Site Overview**

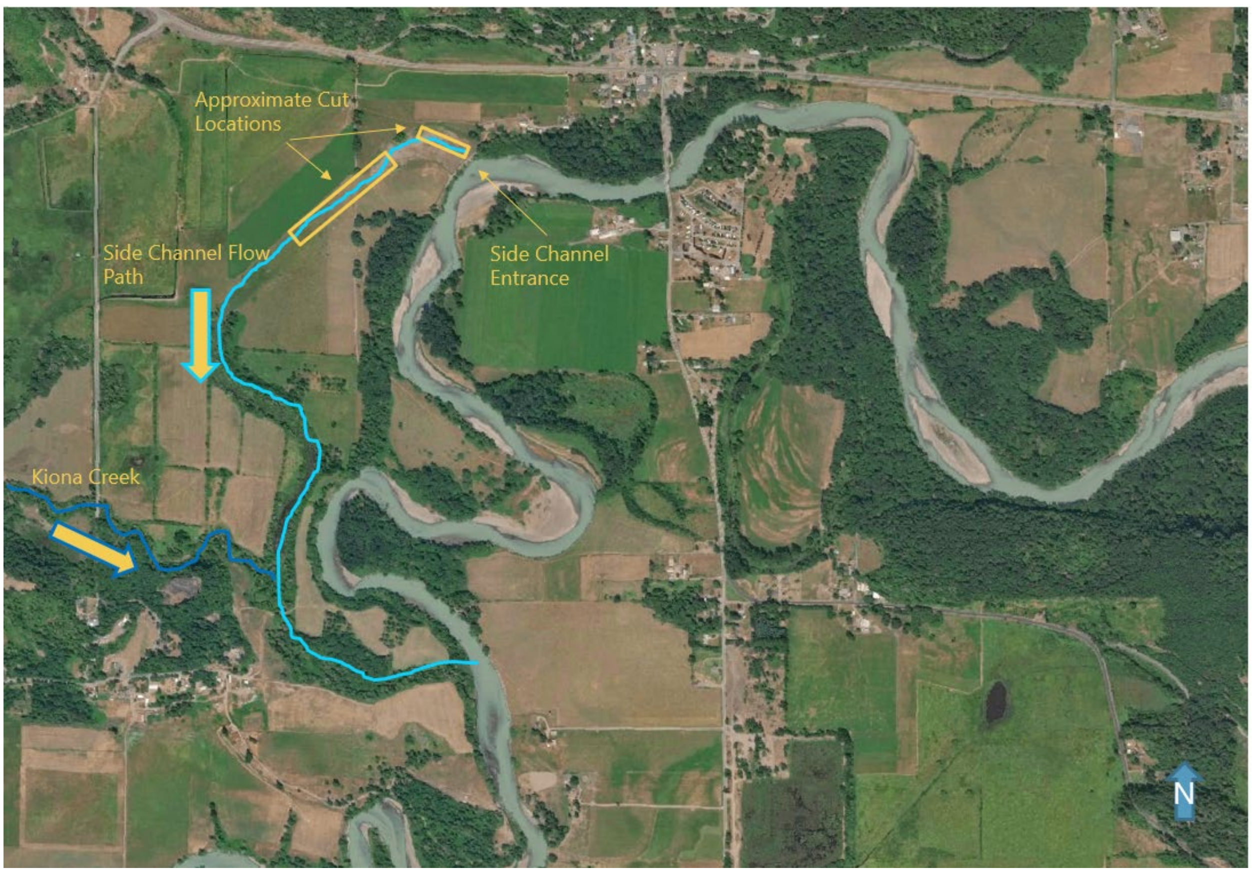

## Model Changes

USACE HEC-RAS version 5.0.5 was used as the modeling framework and the model was composed of both 1D and 2D sections. A terrain representing existing conditions was composed of topo-bathymetric ("blue-green") LiDAR gathered by Quantum Spatial, Inc. in 2018 (QSI 2018) and patched with interpolated elevations from longitudinal profile lines. For a detailed description of the entire model development, see the *Hydrodynamic Modeling and Habitat Suitability Assessment Report* to which this memorandum is appended.

In this modeling effort, three alternative channel cut designs were blended into the existing terrain to create the proposed model surfaces. Alternative 1 included one wide channel cut 140 feet in width to connect the upstream and downstream portions of the side channel. The cut in Alternative 2 followed the same trajectory as Alternative 1, but with a reduced width of 50 feet and a reduced cut length with the goal of limiting earthwork. Alternative 3 maintained a similar downstream cut to Alternative 2 and added an additional cut at the side channel's upstream entrance with the objective of inundating the channel at a more frequent return interval. Alternative 3 also lowered the elevation of the lower cut to connect flow at a lower return interval. The three alternatives are displayed along with the existing conditions in Figure 2.

The model's 2D grid was refined in the region of the side channel to improve resolution for this analysis. In addition to grid refinement, the Manning's *n* layer for the model was updated for the excavated side channel to match the existing value of 0.12 for "Woody Wetlands" in the lower side channel, which accounts for wood roughness in an open channel. Following updates, all four model runs were completed using the unsteady flow file, which contained simulated hydrographs for consecutive 2-year and 10-year floods in the upper Cowlitz basin.

Figure 3 shows a cross section profile comparison for two locations on the side channel comparing the existing conditions topography to Alternative 3.

**Figure 2**
**Existing vs. Alternative Channel Terrains**

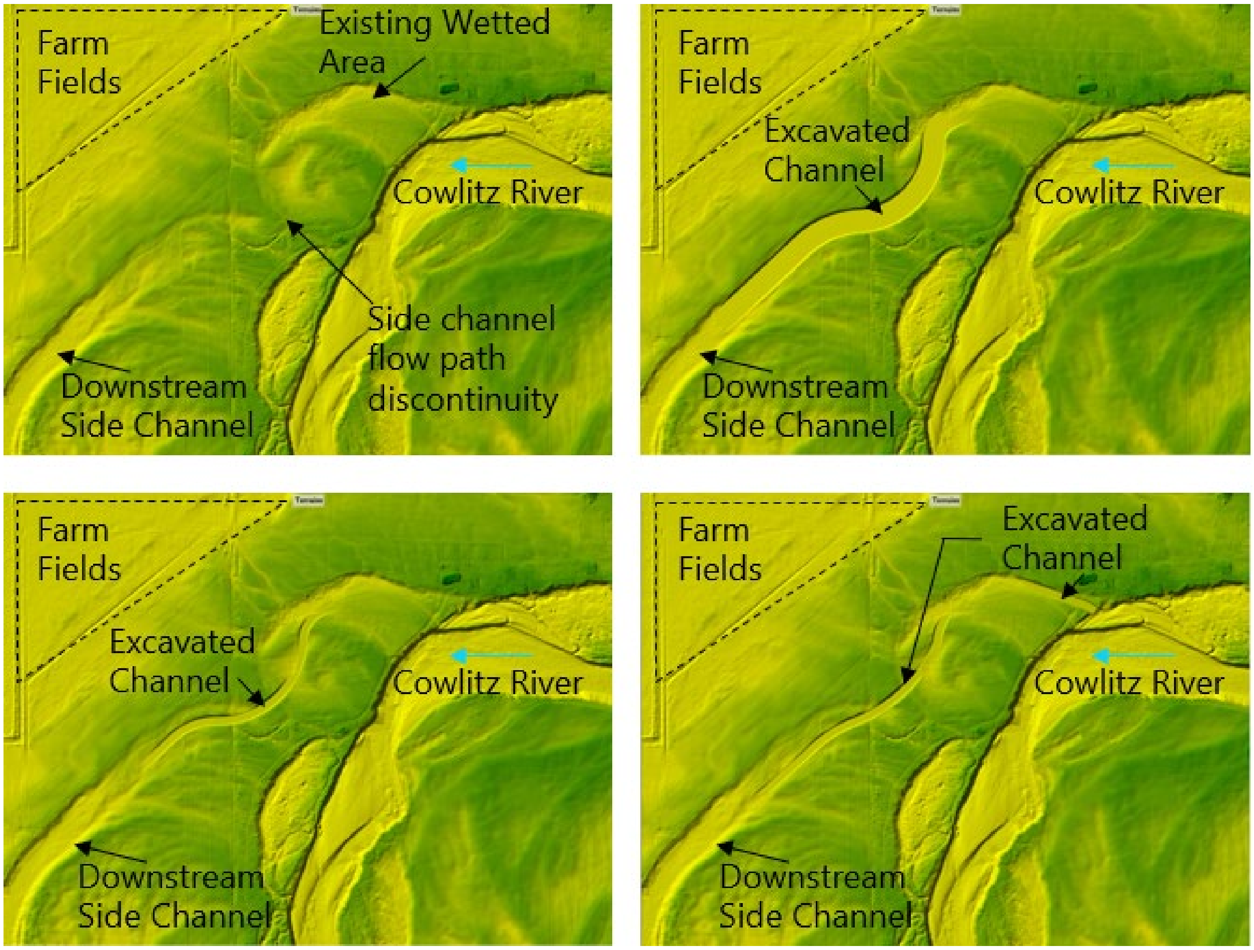


Existing Conditions (Top Left), Alternative 1 (Top Right), Alternative 2 (Bottom Left), Alternative 3 (Bottom Right)

**Figure 3**
**Randle Channel Cross Section Profile Comparison**

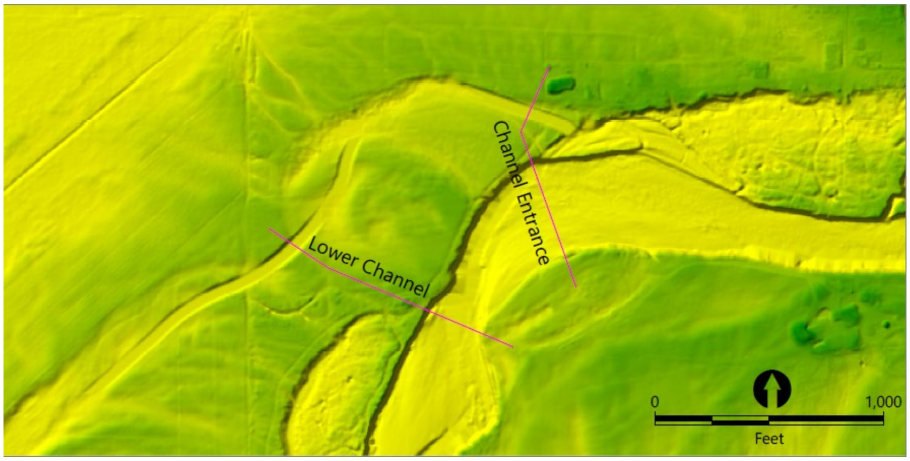


Terrain Profile on "Channel Entrance"

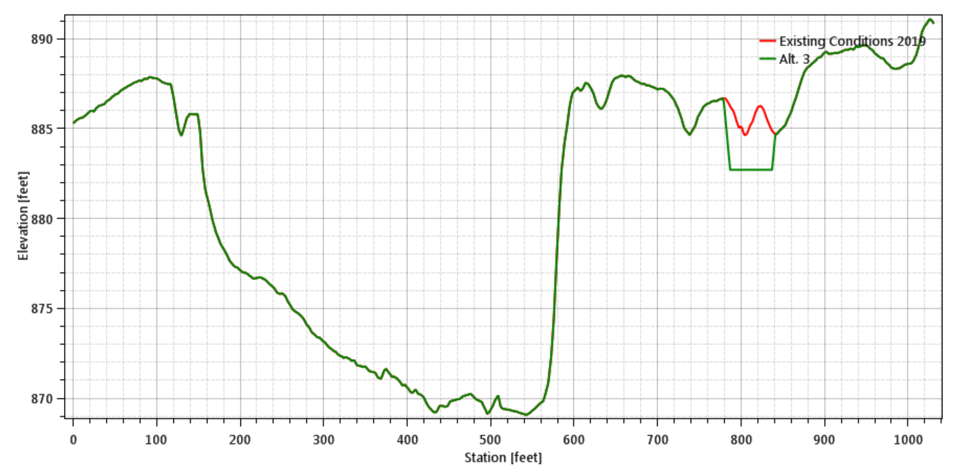


Terrain Profile on "Lower Channel"

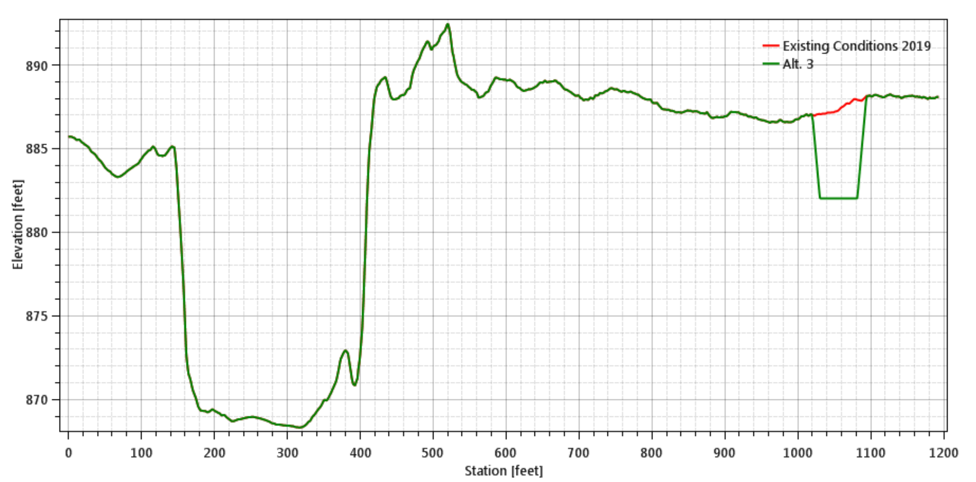


Note: Elevations shown are in feet NAVD88 vertical datum.

## Flood Return Interval Analysis

Hydrologic data containing peak flood return intervals were downloaded from the USGS StreamStats database and used to create a return interval regression for this location on the Cowlitz River at Randle (USGS 2020). The 2-, 5-, 10-, 25-, 50-, 100-, 200-, and 500-year flood values developed in StreamStats using hydrologic parameters such as basin size and precipitation data were plotted on a log-log plot, which related discharge and return interval. The resulting logarithmic trendline equation was used to calculate approximate return intervals for given discharges output from the HEC-RAS model. Return intervals were also checked using a Log Pearson Type III approach to generate a flood frequency curve using the water year 1994 to 2018 peak flow data from the USGS flow gauge at Randle (USGS 2020b). Because the dataset from the Randle gauge had a relatively small sample size, the regression generated from the StreamStats data was used to generate flood return intervals for this analysis.

# Results

Results were generated for the proposed alternatives and existing conditions for multiple parameters including flow depth, water surface elevation, velocity, and shear stress. Model results snapshots were taken at relevant intervals including the minimum discharge that resulted in connected flow throughout the side channel, the discharge that resulted in connected flow into the adjacent farm fields, and the depth of peak inundation for the 2-year and 10-year simulated floods. HEC-RAS was also used to generate maximum velocity and shear stress maps, which displayed the maximum values at each location throughout model time.

## Relevant Hydrologic Snapshots

The following tables and figures display snapshots of critical moments during each model run including the minimum flow that hydraulically connected the side channel, the minimum flow that resulted in hydraulically connected flooding of the farm fields northwest of the side channel, and the maximum inundated extents of the 2- and 10-year simulated floods. Tables 1 and 2 show the river's discharge when connected flow and farm flooding occurred, and the same data are represented graphically in Figure 4.

**Table 1**
**Minimum Discharge that Resulted in Connected Flow Through the Side Channel**

| Model Run | Cowlitz River Discharge at Randle (cfs) | Estimated Return Interval (years) |
|---|---|---|
| Existing Conditions | 25,320 | 4.8 |
| Alternative 1 | 17,485 | 2.4 |
| Alternative 2 | 18,375 | 2.6 |
| Alternative 3 | 14,518 | 1.8 |

**Table 2**
**Discharge that Resulted in Connected Flooding of the Farm Fields**

| Model Run | Cowlitz River Discharge at Randle (cfs) | Estimated Return Interval (years) |
|---|---|---|
| Existing Conditions | 18,900 | 2.7 |
| Alternative 1 | 22,225 | 3.6 |
| Alternative 2 | 20,718 | 3.2 |
| Alternative 3 | 19,908 | 3.0 |

**Figure 4**
**Discharges of Side Channel Connected Flow and Flooding of Farm Fields**

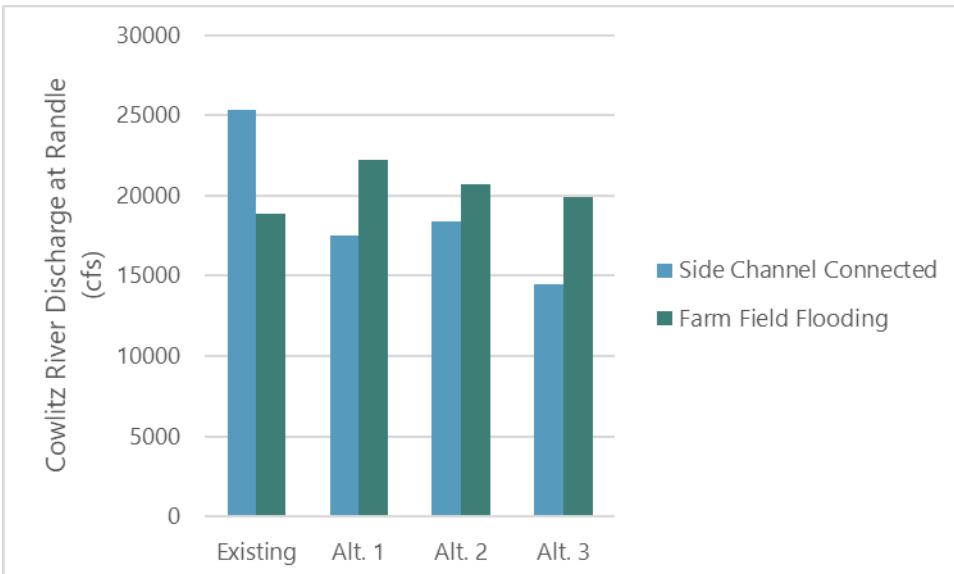


Results show that the existing conditions required a larger return interval of 4.8 years to hydraulically connect the side channel, while Alternatives 1, 2, and 3 required approximately 2.4-, 2.6-, and 1.8-year return intervals to achieve the same connection. All the proposed channels significantly reduced the flow required to connect the side channel because of the addition of the lower channel cut. Alternative 3 resulted in connected flow at a particularly low return interval because the side channel entrance was lowered with the addition of the upper cut and the elevation at the top of the lower cut was also lowered.

The discontinuity in the side channel in the existing conditions explains why the farm fields flooded at a lower return interval than the proposed alternatives. Alternative 1 showed the greatest ability to buffer against flooding of the farm fields due to the wider channel cut, which could convey more flow to the lower side channel than the other alternatives. Alternative 3 resulted in flooding of the fields at the lowest return interval among the three alternatives because the side channel entrance was lowered.

Figures 5 and 6 provide screenshots of the model time steps when both conditions were achieved for each alternative. These figures demonstrate that the existing conditions lack a path for water to connect to the lower side channel, resulting in extensive flooding of the farm fields before this occurs. All the alternatives remedy this discontinuity with a channel cut, allowing the connection to be made before water backed up into the farm fields.

**Figure 5**
**Water Depth at Connected Flow Through Side Channel**

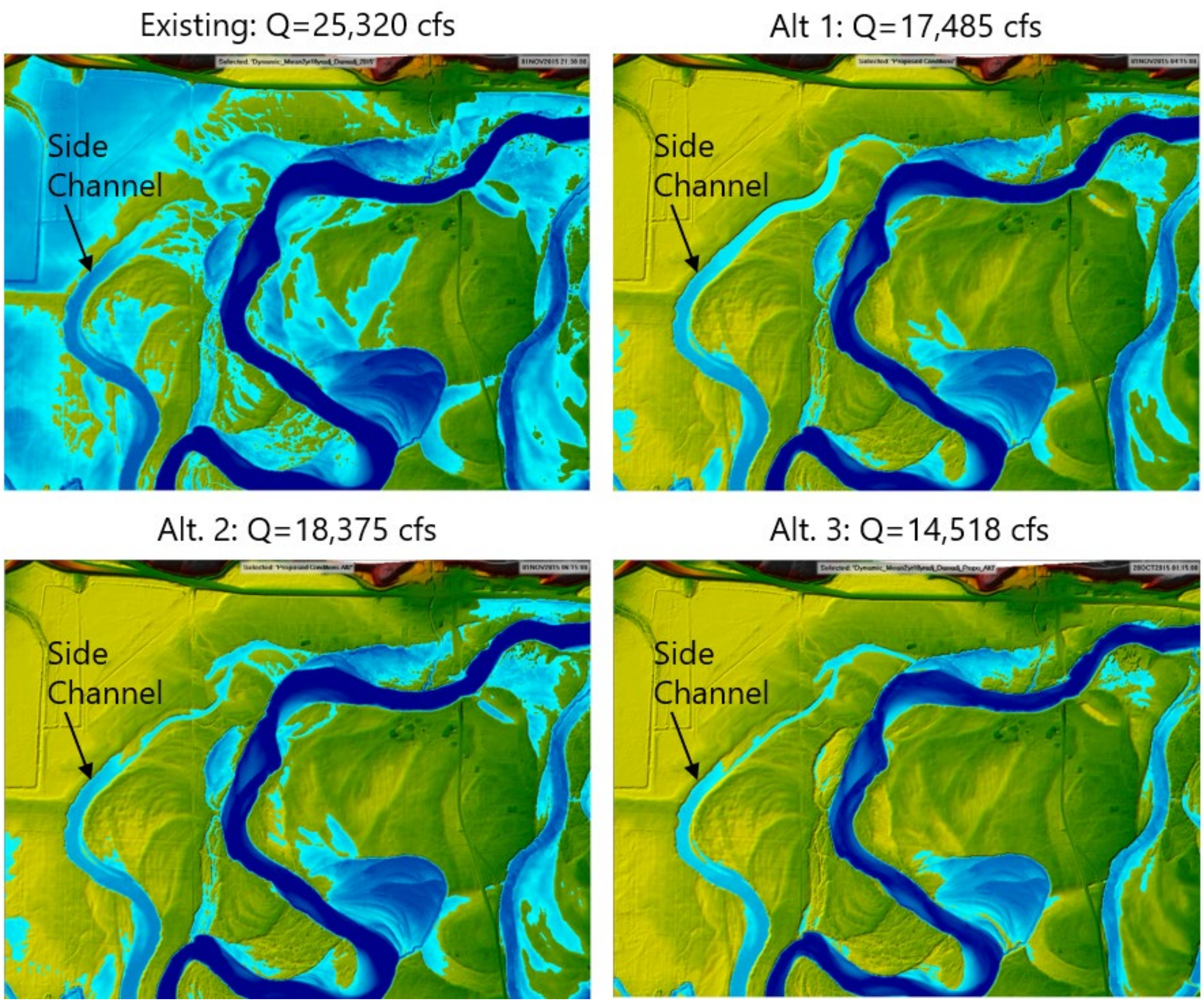

**Figure 6**
**Water Depth at Inundation of Farm Fields**

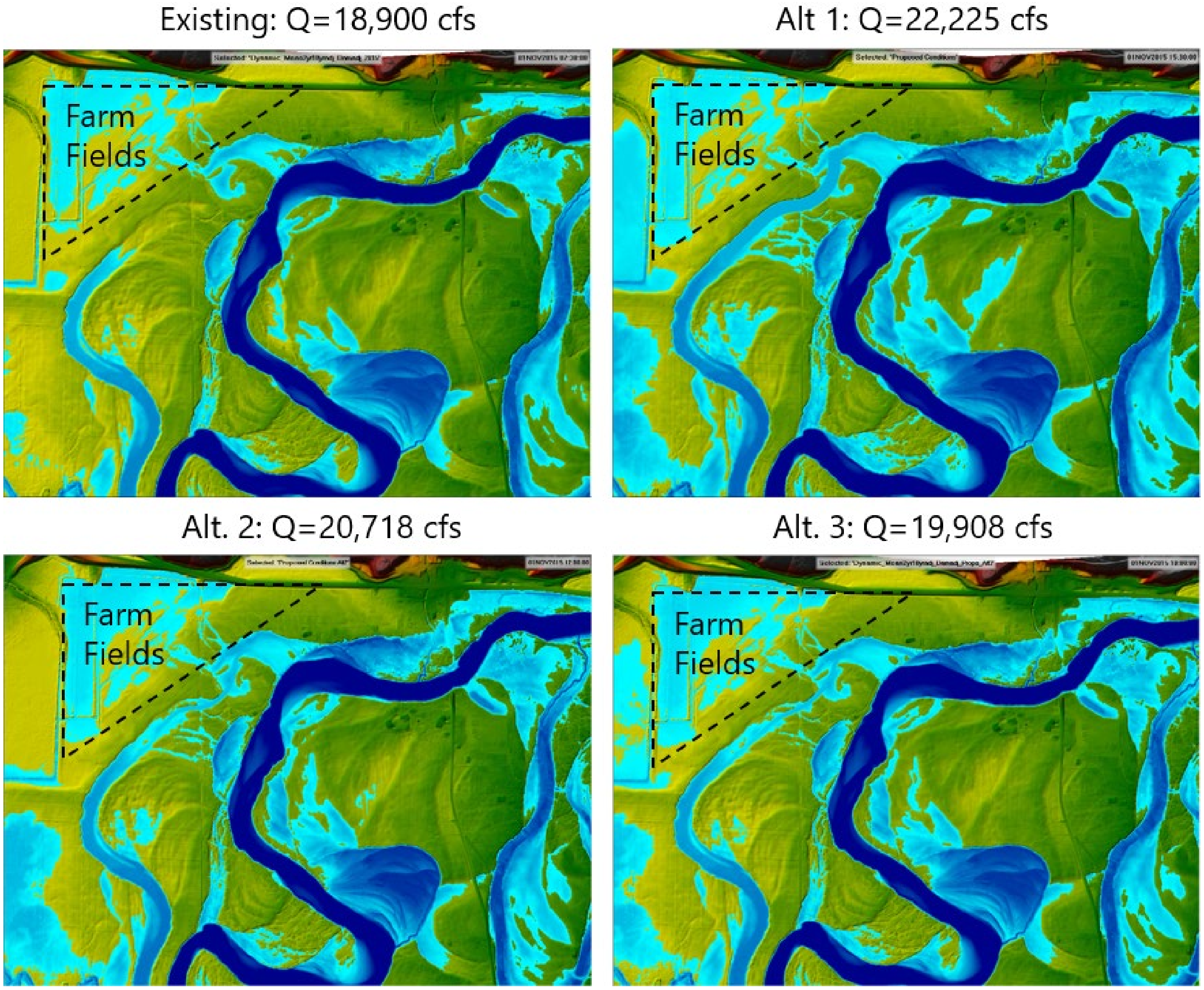


Figures 7 and 8 show the maximum flooded extents during the 2-year and 10-year simulated floods. The 2-year and 10-year simulated events have maximum discharges of approximately 16,525 and 27,225 cfs for the entire river at the entrance of the side channel. Figure 7 shows that the side channel is not connected in the existing conditions during the 2-year event, while the proposed alternatives each result in connected flow. Figure 7 also shows some flooding in the farm fields for Alternative 3 during the 2-year flood; however, this water is hydraulically disconnected from the rest of the flow and is the result of an error in the model. Manual inspection of model results showed that Alternative 3 did not result in connected flooding of the farm fields until the 3.0-year return interval, which was a slightly larger flow than the 2.7-year event that connected flow to the farm fields in the existing conditions (see Table 2).

**Figure 7**
**Water Depth (feet) During a Modeled 2-Year Peak Flow (16,525 cfs)**

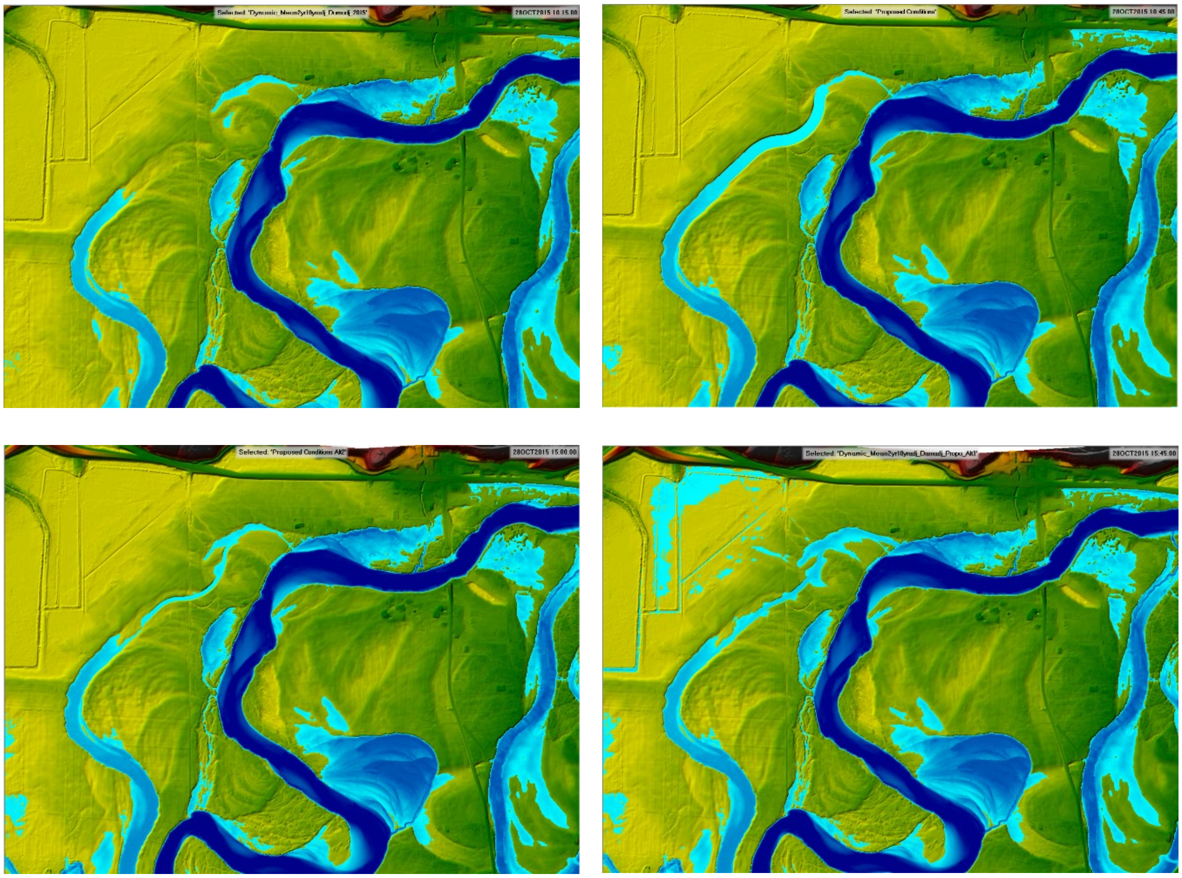

Existing Conditions (Top Left), Alternative 1 (Top Right), Alternative 2 (Bottom Left), Alternative 3 (Bottom Right)

Figure 8 shows that none of the proposed alternatives change the current flooding extent during the 10-year flood. The discharge at this return interval overtops the banks of the side channel regardless of the proposed design and results in similar flooding extents in the existing conditions and all three alternatives.

**Figure 8**
**Water Depth (feet) During a Modeled 10-Year Peak Flow (27,225 cfs)**

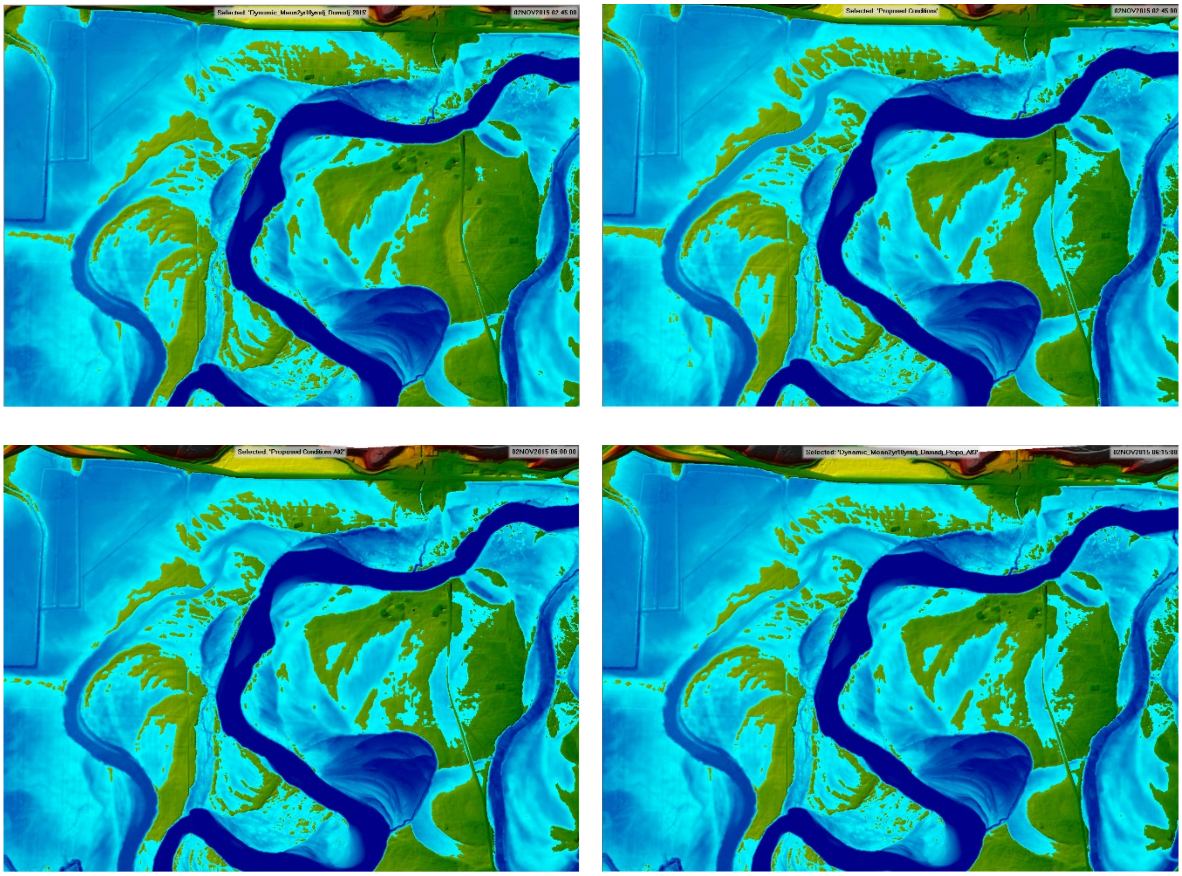

Existing Conditions (Top Left), Alternative 1 (Top Right), Alternative 2 (Bottom Left), Alternative 3 (Bottom Right)

## Flow Velocity

The raster data for maximum velocities throughout model time was output from HEC-RAS and analyzed in GIS to determine maximum values in key regions of interest to this design. These maximum velocities were observed during the rising limb of the 10-year simulated hydrograph before peak inundation extent was reached. The results from the maximum velocity output are shown in Table 3 and Figure 9. These velocities do not consider any large wood potentially added to the side channel, but Manning's *n* values reflect that of a natural channel with wood present. Within the side channel area, high velocities can be observed in the rills connecting the side channel to the low-lying farm fields, and at the entrance to the side channel.

Table 3 shows that the existing conditions had the greatest velocities in all three locations and Figure 9 shows that the high velocity zones at the entrance of the farm fields are largest for the existing conditions. Among the alternatives, Alternative 1 had the highest velocities at the channel entrance but lower velocities into the farm fields and on the designed cut surface. This could be explained by the greater cut width in Alternative 1, which allows a greater discharge to be conveyed to the lower side channel, reducing flow directed towards the farm fields. Alternative 3 had higher velocities into the farm fields than the other two alternatives but lower than the existing conditions. Alternative 3 also had the highest velocity on the proposed cut surface. This velocity of 3.5 ft/s occurred at the downstream end of the channel cut on the left bank, and the high velocity causing this result is due to a rill that connects flow directly from the main channel. This higher velocity path is observed in all conditions, but Alternative 3 picked up more of this velocity within the channel cut due to a slight shift in alignment towards the main channel. See Figure 9, bottom right, for the location of this incoming flow path (circled in red).

**Table 3**
**Maximum Velocities in Key Locations**

| Existing Conditions | | Alternative 1 | | Alternative 2 | | Alternative 3 | |
|---|---|---|---|---|---|---|---|
| **Location** | **Max Velocity (ft/sec)** | **Location** | **Max Velocity (ft/sec)** | **Location** | **Max Velocity (ft/sec)** | **Location** | **Max Velocity (ft/sec)** |
| Channel Entrance | 4.2 | Channel Entrance | 3.1 | Channel Entrance | 2.9 | Channel Entrance | 2.8 |
| Into Farm Field | 5.4 | Into Farm Field | 4.5 | Into Farm Field | 5.0 | Into Farm Field | 5.0 |
| Within Side Channel | 2.7 | Lower Channel Cut | 2.3 | Lower Channel Cut | 2.4 | Both Channel Cuts | 3.5 |

**Figure 9**
**Maximum Velocity (ft/s)**

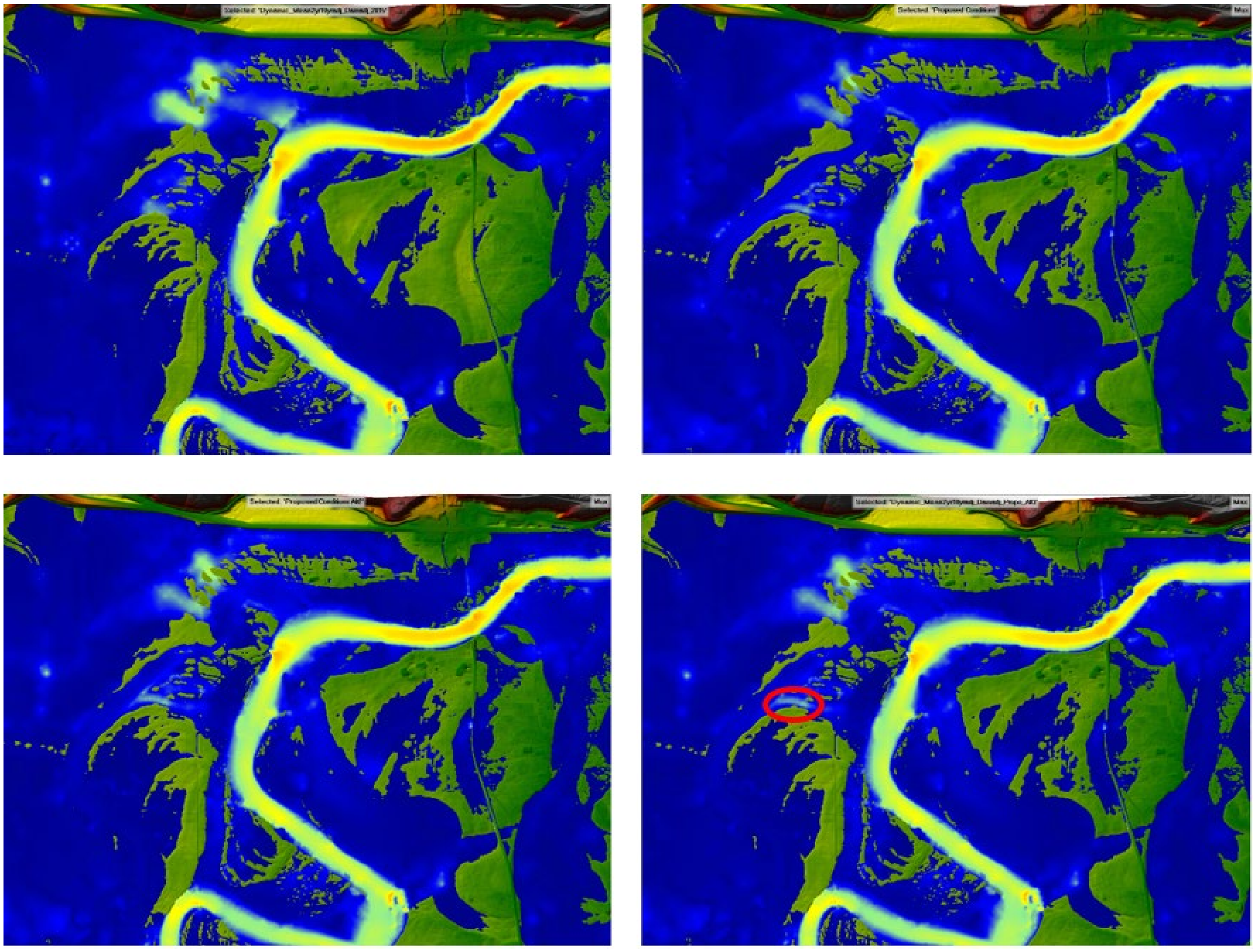

**LEGEND:**

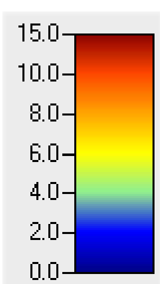


Existing Conditions (Top Left), Alternative 1 (Top Right), Alternative 2 (Bottom Left), Alternative 3 (Bottom Right)

## Shear Stress

The raster data for maximum shear stress throughout model time was similarly output from HEC-RAS and analyzed in GIS to determine maximum values in key regions of interest to this design. The results for maximum shear stress are shown in Table 4 and Figure 10. In addition, shear stress results were output during the peak of the 10-year flood and shown in Figure 11. Results show the design alternatives have greater shear stress values than the existing conditions, which could be a result of increased conveyance in the alternatives due to the channel cuts. Shear stress values into the farm fields are comparable between the existing conditions and alternatives; however, the alternatives show greater peak shear stress, specifically on the right bank or inside edge of the lower channel cut. These higher shear stress values are likely a result of the earthwork which introduced planar bank slopes to the previously smooth terrain. Figure 10 shows that the relative maximum shear stress in the channel is low compared to the peak shear stress values on the inside edges of bends in the main channel. The purpose of this comparison is to show that the proposed side channel excavation alternatives are not responsible for creating zones of greater shear stress than the existing main channel. Figure 11 also shows a zone of increased shear stress in for the alternatives relative to existing conditions at the channel entrance. This could indicate a potential scour zone as the material at entrance of the overflow channel is moved to reach equilibrium with the grade of the downstream cut.

**Table 4**
**Maximum Shear Stress Values in Key Locations**

| Existing Conditions | | Alternative 1 | | Alternative 2 | | Alternative 3 | |
|---|---|---|---|---|---|---|---|
| **Location** | **Max Shear Stress ($lb/ft^2$)** | **Location** | **Max Shear Stress ($lb/ft^2$)** | **Location** | **Max Shear Stress ($lb/ft^2$)** | **Location** | **Max Shear Stress ($lb/ft^2$)** |
| Channel Entrance | 0.7 | Channel Entrance | 1.8 | Channel Entrance | 1.8 | Channel Entrance | 1.7 |
| Into Farm Field | 0.4 | Into Farm Field | 0.3 | Into Farm Field | 0.4 | Into Farm Field | 0.4 |
| Within Side Channel | 0.3 | Lower Channel Cut | 1.8 | Lower Channel Cut | 0.8 | Both Channel Cuts | 0.9 |

**Figure 10**
**Maximum Shear Stress (lb/ft$^2$)**

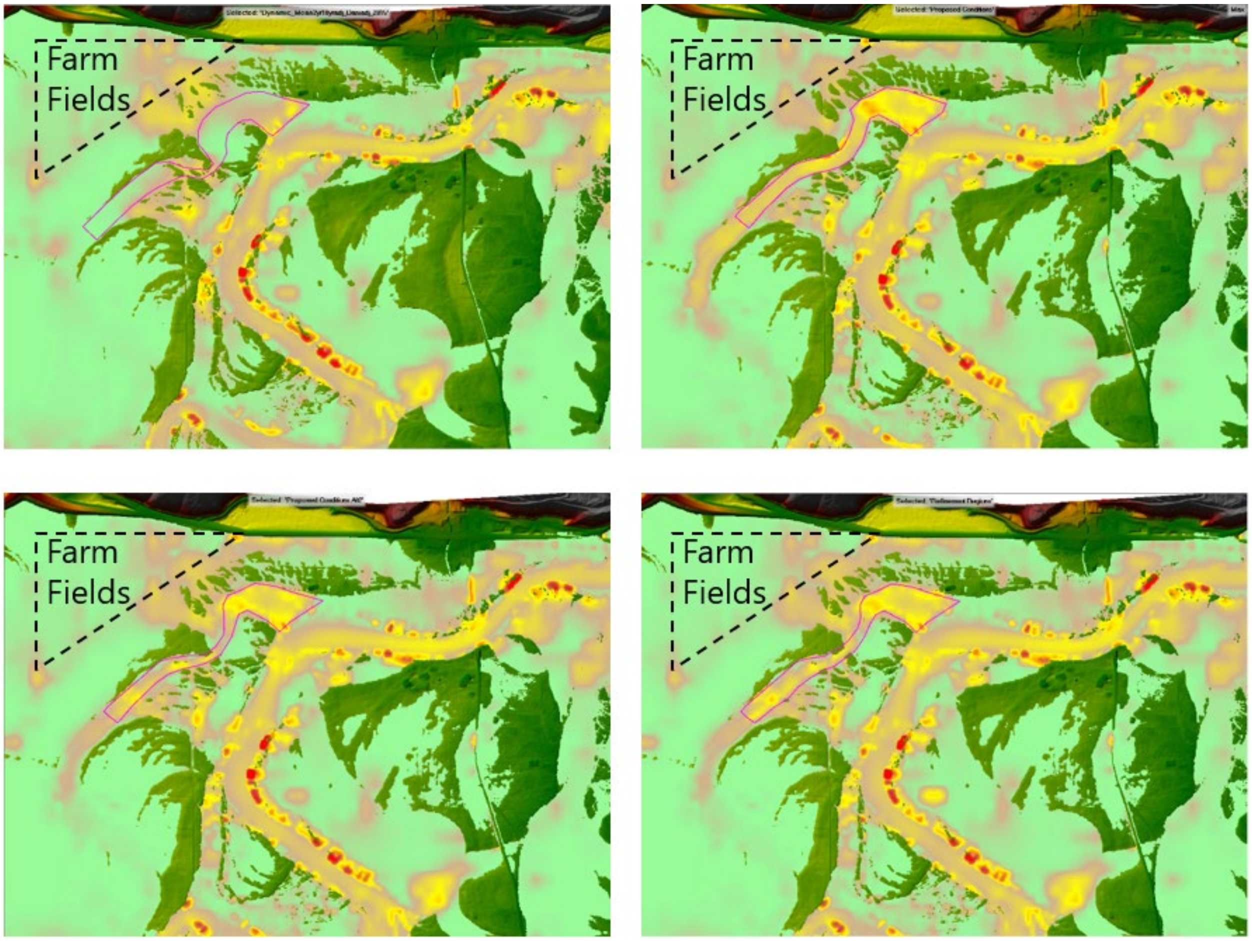


**LEGEND:**

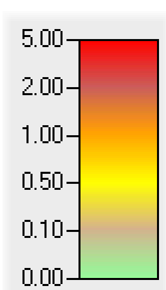


Existing Conditions (Top Left), Alternative 1 (Top Right), Alternative 2 (Bottom Left), Alternative 3 (Bottom Right). Side channel highlighted in pink.

**Figure 11**
**10-Year Peak Flow (27,225 cfs) – Shear Stress**

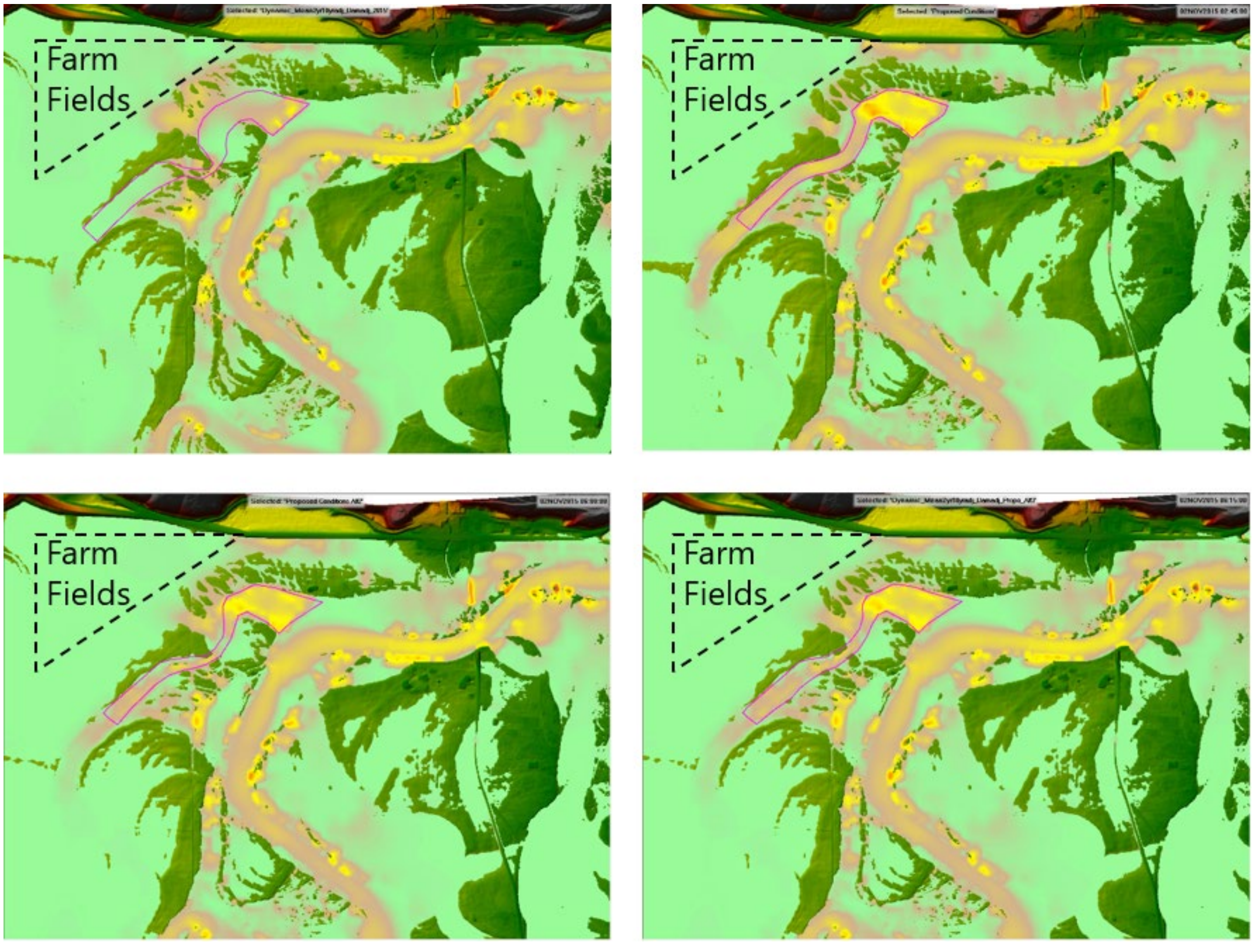


**LEGEND:**

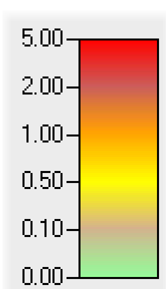


Existing Conditions (Top Left), Alternative 1 (Top Right), Alternative 2 (Bottom Left), Alternative 3 (Bottom Right). Side channel highlighted in pink.

## Summary of Findings

The modeling results demonstrate that the proposed alternatives help increase the frequency of continuous flow through the side channel. The connection was improved by cutting a flow path between the upper and lower sections of the side channel. In the current conditions, flow backs up in the upper side channel, causing flooding of the farm fields at approximately the 2.7-year return interval flow. The proposed conditions alleviate this backwater and postpone flooding of the farm fields from a range of the approximately 3- to 3.6-year return interval flows. Creating a flow path through the side channel also results in continuous flow during the 2-year flood for each of the alternatives. In the existing conditions, the 2-year flood caused pooling in the side channel and flow did not connect to the downstream portion of the existing side channel until approximately the 4.8-year flood. Alternatively, results from the 10-year flow show no improvement in inundation extent for the proposed alternatives compared to existing conditions.

Among the proposed alternatives, Alternative 1 has the greatest capacity to buffer against flooding in the farm fields due to increased channel cut width, while Alternatives 2 and 3 reduce some of this capacity to prevent flooding of the farm fields. Alternative 3 greatly reduces the return interval required for connected flow in the side channel by adding an additional cut at the side channel entrance, but this cut also reduces the capacity of Alternative 3 to buffer against flooding of the farm fields relative to the other alternatives.

Results for flow velocity indicate some changes resulting from more flow being routed through the side channel in the proposed alternatives. Results indicate reduced maximum velocities at the channel entrance and the entrance to the farm fields for Alternatives 1 and 2 compared to existing conditions. Alternative 3 shows reduced maximum velocities relative to the other alternatives at the channel entrance but slightly higher velocities into the farm fields and within the proposed cut surface. Overall, the alternatives help reduce the velocities into the farm fields by opening the hydraulic connection to the lower side channel.

Shear stress results highlight important design considerations. Shear stress values for all three alternatives are higher than the existing conditions at the entrance to the overflow channel and within the side channel. These higher shear stress values span a region between the main channel and the beginning of our designed channel cut, indicating a potential scour zone as the material at the crest of the overflow channel reaches equilibrium with the designed channel grade.

## Considerations for Design

Modeled results reveal some key areas to consider during the continuing design process. The first is that the farm fields adjacent to the overflow channel lie 1 to 2 feet below the base of the side channel at the location where flow enters the fields. Currently, Alternative 3 is the best option to maximize connectivity of the side channel at the lowest return intervals but it reduces flooding of the farm fields less than the other alternatives. Results from Alternatives 1 and 2 show that changing the width of the channel cut varies the return interval that causes flooding in the farm fields. Together, results show that there is opportunity to optimize a cost-feasible design to maintain the increased side channel connectivity of Alternative 3 while increasing the channel's resistance to flooding the farm fields. To help meet the design goal of reducing flooding, logs and fill material could be added in the rills that connect the side channel to the fields. Additionally, logs and woody debris additions would help create high flow refugia for salmonids.

The second consideration apparent in the model is the need to assess the effects of potential scour at the entrance of the overflow channel in the proposed conditions. The current zone of higher shear stress indicated in the alternatives could indicate scour or headcutting at the upstream entrance to the overflow channel. This would potentially lower the flow that enters the channel, which may be beneficial from a habitat perspective, but may contribute to additional flooding of the farm fields. Precautions such as large woody debris and engineered log jams could be implemented to deal with this natural regrading and mitigate against additional flooding.

## References

Lower Columbia Fish Recovery Board, 2019. *Upper Cowlitz & Cispus Habitat Strategy*. December 2019. Available at: https://www.lcfrb.gen.wa.us/upper-cowlitz-cispus-work-group.

QSI, 2018. *Cowlitz River, Washington Topobathymetric LiDAR Technical Data Report*. July 20, 2018.

USGS (U.S. Geological Survey), 2020a. *StreamStats in Washington*. Available at: https://streamstats.usgs.gov/ss/.

USGS, 2020b. USGS 14231000 Cowlitz River at Randle, WA. Available at: https://waterdata.usgs.gov/nwis/uv?site_no=14231000.